

# THEORETICAL CHEMISTRY INSTITUTE

## THE UNIVERSITY OF WISCONSIN

SEARCHED \_\_\_\_\_

INDEXED (S) \_\_\_\_\_

Hard copy (HC)

Microfiche (MF)

6-653 July 65

### SUDDEN APPROXIMATION APPLIED TO ROTATIONAL EXCITATION OF MOLECULES BY ATOMS. II. SCATTERING OF POLAR DIATOMICS

by

R. B. Bernstein

and

K. H. Kramer

WIS-TCI-91

13 July, 1965

ACQUISITION FORM 602

(ACQUISITION NUMBER)	73
(PAGE(S))	1
CR 67044	
(NASA CR OR TMN OR AD NUMBER)	13001
(CODE)	13001
(CATEGORY)	1

MADISON, WISCONSIN

SUDDEN APPROXIMATION APPLIED TO ROTATIONAL EXCITATION OF  
MOLECULES BY ATOMS. II. SCATTERING OF POLAR DIATOMICS  $\nabla$

by

R. B. Bernstein and K. H. Kramer

Theoretical Chemistry Institute, University of Wisconsin

Madison, Wisconsin 53706

ABSTRACT

3400

The sudden approximation is applied to the computation of rotational transition probabilities and inelastic total cross sections for the scattering of polar and non-polar diatomic molecules (rigid rotors) by atoms. The calculations are based upon an interaction potential which includes both short- and long-range anisotropies. At thermal energies the long-range attractive parts of the potential are of principal importance in determining the inelasticity, with the main contribution arising from the quadrupole interaction term (varying as  $R^{-7} \cos^3 \theta$ ). The computations show the rapid onset of "dominant-coupling" behavior (randomization of transition probability among all close-coupled states) for impact parameters below about  $(S/\pi)^{\frac{1}{2}}$ , where  $S$  is the total inelastic total cross section.

*Author*

$\nabla$  Supported principally by National Aeronautics and Space Administration, Grant NsG-275-62, with partial support from Applied Physics Lab. Subcontract No. 181461, Bureau of Naval Weapons, (Govt. Prime Contract N0w 62-0604-c).

$\nabla$  Present Address: Physikalisches Institut der Universität,  
Freiburg/i. Br., Germany.

## 1. Introduction

In paper I<sup>1</sup> the sudden approximation was applied to the problem of evaluating transition probabilities and cross sections for rotational excitation and scattering of homonuclear diatomic molecules by atoms. The approach was based upon the Alder-Winther<sup>2</sup> theory of Coulomb excitation, taken in its simplest form. The analysis was restricted to low-angle scattering, sensitive primarily to the long-range attractive part of the potential and its anisotropy.

Although the results of I were of limited practical value due to the neglect of the short-range repulsive interactions, they served to illustrate the main features of the sudden approximation as applied to the problem of rotational excitation of molecules. It was noted that calculated transition probabilities do not exceed unity, and that the results reduce properly in the weak-interaction limit to those of conventional first-order perturbation theory.

It was also seen (in accord with expectation<sup>3</sup>) that with increasing strength of interaction the "selection rules" become progressively weakened, and more and more "forbidden" channels open up. In this process, the individual transition probabilities become essentially randomized, with expectation values given by the reciprocal of the number of open channels<sup>3</sup>.

- - - -
1. K. H. Kramer and R. B. Bernstein, J. Chem. Phys. 40, 200 (1964), hereafter referred to as I.
  2. K. Alder and A. Winther, Kgl. Danske Vidensk. Selsk. Mat.-fys. Medd. 32, No. 8 (1960).
  3. R. B. Bernstein, A. Dalgarno, H. S. W. Massey and I. C. Percival, Proc. Roy. Soc. (London), A274, 427 (1963).

The present work (II) is / <sup>extended to</sup> the more general case of collisions of heteronuclear diatomic molecules with atoms, taking account of the repulsive as well as the attractive parts of the potential, and thus the large-angle scattering associated with "strong" collisions.

The treatment is, of course, an approximation, expected to be valid only under certain restrictive conditions. The principal assumption is that of the validity of the sudden approximation per se; a number of additional simplifying assumptions have been introduced to make the computations tractable. Within the limitations imposed by these assumptions (which are detailed below and which may be considered to define the present model) the treatment is rigorous.

## 2. Assumptions

(1) The sudden approximation: strictly valid <sup>V</sup> only in the limit when the perturbation Hamiltonian  $\hat{H}'(t)$  commutes with  $\hat{H}_0$ , the unperturbed rotor Hamiltonian. In the interaction picture <sup>V</sup> the Schrödinger equation

$$i\hbar \frac{\partial \Psi(t)}{\partial t} = [\hat{H}_0 + \hat{H}'(t)] \Psi(t) \quad (1)$$

- - - - -  
4. See, for example, E. Merzbacher, "Quantum Mechanics", J. Wiley and Sons, N.Y. 1961, Chap. 19; A. Messiah, "Quantum Mechanics", J. Wiley and Sons, N.Y. 1962, Chap. 17.

becomes

$$i\hbar \frac{\partial U(t, t_0)}{\partial t} = \hat{V}_I(t) U(t, t_0) \quad (2)$$

where  $U(t, t_0)$  is the propagator and

$$\hat{V}_I(t) = e^{\frac{i}{\hbar} \hat{H}_0 t} \hat{H}'(t) e^{-\frac{i}{\hbar} \hat{H}_0 t} \quad (3)$$

Thus in the limit when  $[\hat{H}_0, \hat{H}'(t)] = 0$ ,

$$\hat{V}_I(t) = \hat{H}'(t) = V(t), \quad (4)$$

where  $V$ , the interaction potential, is the perturbation, so that

$$U(t, t_0) = e^{-\frac{i}{\hbar} \int_{t_0}^t V(t') dt'} \quad (5)$$

and

$$P(\beta, \alpha) = |\langle \beta | U(\infty, -\infty) | \alpha \rangle|^2. \quad (6)$$

As in I,  $P(\beta, \alpha)$  is the  $\alpha \rightarrow \beta$  transition probability.

Strictly speaking, the requirement<sup>2,5/</sup> that the commutator  $[\hat{H}_0, \hat{H}'(t)]$  must vanish demands that all the energy levels of the unperturbed system be degenerate, i.e., that  $E_\beta - E_\alpha = 0$

5. D. W. Robinson, Helv. Phys. Acta 36, 140 (1963).

for all  $\alpha, \beta$ . However, it is usually assumed  $\checkmark$  that Eq. 6 is applicable if, for the particular levels considered,

$$\frac{|E_\beta - E_\alpha|}{\hbar} \ll \tau_c^{-1}, \quad (7)$$

where  $\tau_c$  is some characteristic "collision-time" (for example, we may consider  $\tau_c \approx \sigma/v_0$  where  $\sigma$  is the collision diameter and  $v_0$  the incident relative velocity). In other words, the "collision time" is assumed short compared to the classical rotation period of the molecule.

As in I, Eq. 6 is used in the form

$$P(j'm'; jm | b, E) = |\langle j'm' | e^{-i \int_{-\infty}^{\infty} V(t) dt} | jm \rangle|^2 \quad (8)$$

where  $j, m$  and  $j', m'$  are the initial and final values, respectively, of the rotational and magnetic (projection) quantum numbers of the rotor. As before, the matrix element is evaluated directly by quadrature, without approximation.

(2) Classical trajectory: in order to evaluate the action integrals needed in connection with Eq. 8, a simplified classical trajectory is employed, based upon an assumed central (orientation-averaged) interaction potential. For this purpose, the convenient two-parameter L.-J.(12,6) form has been adopted:

$$\bar{V}(R) = C^{(12)} \cdot R^{-12} - C^{(6)} \cdot R^{-6} \quad (9)$$

where the symbols have their usual meanings. Such a central potential, of course, implies a planar trajectory in the center-of-mass system (the plane is chosen such that  $\phi' = 0$  in Fig. 1 of I). Yet it is obvious that  $m$ -transitions necessarily introduce an out-of-plane component to the motion. Fortunately, the dihedral angle between "incident" and "outgoing" planes is usually quite small ( $\approx |\Delta m|/bk \ll 1$ ) for the physical situation under consideration<sup>1</sup>, i.e., "fast" collisions of heavy particles (high  $k$ ), molecules in low  $j$  states, and not-too-small impact parameters (b)<sup>6</sup>.

(3) Form of the angle-dependent interaction potential: it is desirable to choose the simplest functional form which can describe both the long-range attraction with its angular anisotropy and a short-range repulsion with appropriate asymmetry. For this purpose the following atom-molecule potential has been adopted, which, upon orientation-averaging, reduces to the simple L.-J.

(12,6) form (Eq. 9):

$$V(R, \theta) = C^{(12)} R^{-12} [1 + b_1 P_1(\cos \theta) + b_2 P_2(\cos \theta)] - C^{(6)} R^{-6} [1 + a_2 P_2(\cos \theta)] - C^{(7)} R^{-7} \left[ \frac{3}{5} P_1(\cos \theta) + \frac{2}{5} P_3(\cos \theta) \right] \quad (10)$$

- 
6. Thus, if  $J = \ell + j$  represents the total angular momentum (conserved in the collision), then for low  $j$  and the usually large  $\ell$  ( $\ell \gg j$ ),  $J \approx \ell \approx bk \gg j$ ;  $|\Delta m| < 2|\Delta j|$  and  $|\Delta m| \ll bk$ .

Here  $\Theta$  is the angle between  $\tilde{R}$  and the molecular axis,  $C^{(12)} = 4 \epsilon \sigma^{12}$ ,  $C^{(6)} = 4 \epsilon \sigma^6$ ,  $C^{(7)} = 6 \alpha \mu Q \sqrt{\epsilon}$ ;  $\epsilon$  and  $\sigma$  are the L.-J. (12,6) well-depth and size parameters,  $\alpha$  is the atom polarizability,  $\mu$  and  $Q$  the molecular electric dipole and quadrupole moments, respectively. The  $P_n(\cos \theta)$  are Legendre functions. Of the three anisotropy parameters  $a_2$ ,  $b_1$  and  $b_2$ , unfortunately, only one ( $a_2$ ) may be estimated<sup>8</sup> with any degree of reliability. For the homonuclear case, of course, it is assumed that  $b_1 = C^{(7)} = 0$ .

### 3. Action Integrals

In order to evaluate the action integrals, i.e., the integrals over the trajectory needed in Eq. 8, it is convenient to express the equation for the potential in a slightly different form, i.e., to eliminate  $\Theta$  in favor of the angles  $\theta, \phi$  and  $\theta', \phi'$  (refer to Fig. 1 of I). Making use of the addition theorem for spherical harmonics and introducing certain "reduced notation", Eq. 10 may be re-written:

$$\begin{aligned} V(x; \theta, \phi; \theta', \phi') = 4\epsilon & \left\{ x^{-12} \left[ 1 + b_1 \sum_m C_m^{(1)*}(\theta, \phi) C_m^{(1)}(\theta', \phi') + b_2 \sum_m C_m^{(2)*}(\theta, \phi) C_m^{(2)}(\theta', \phi') \right] \right. \\ & - x^{-6} \left[ 1 + a_2 \sum_m C_m^{(2)*}(\theta, \phi) C_m^{(2)}(\theta', \phi') \right] \\ & \left. - x^{-7} \left[ \frac{3c}{5} \sum_m C_m^{(1)*}(\theta, \phi) C_m^{(1)}(\theta', \phi') + \frac{2c}{5} \sum_m C_m^{(3)*}(\theta, \phi) C_m^{(3)}(\theta', \phi') \right] \right\} \end{aligned} \quad (11)$$

- - - - -
7. J. P. Toennies [Z. Physik. 182, 257 (1965)] has shown the need for the Anderson  $R^{-7} \cos^3 \Theta$  anisotropy term.
  8. J. O. Hirschfelder, C. F. Curtiss and R. B. Bird, "Molecular Theory of Gases and Liquids", J. Wiley and Sons, N.Y., 1964 (Second Printing), Chaps. 13 and 14.

where the C function is that of Racah<sup>9</sup>:

$$C_m^{(l)}(\theta, \phi) = \left(\frac{4\pi}{2l+1}\right)^{\frac{1}{2}} Y_l^m(\theta, \phi) , \quad (12)$$

$$x \equiv R/\sigma \quad \text{and} \quad c \equiv C^{(7)} / 4\epsilon\sigma^7 = \frac{3}{2} \alpha \mu Q / \epsilon \sigma^7 . \quad (13)$$

For a given impact parameter b, a "reduced action" G( $\theta, \phi$ ) is defined and evaluated:

$$G(\theta, \phi) = \frac{1}{\hbar} \int_{-\infty}^{\infty} V(t) dt = \frac{2}{\hbar v_0} \int_{R_0}^{\infty} \frac{V(R, \theta) dR}{F(R)} = \frac{2\sigma}{\hbar v_0} \int_{x_0}^{\infty} \frac{V(x; \theta, \phi; \theta', \phi') dx}{F(x)} \quad (14)$$

where use has been made of the relation<sup>10</sup>  $dt = dR/v_0 F(R)$

where

$$F(R) = \left[ 1 - \frac{b^2}{R^2} - \frac{\bar{V}(R)}{E} \right]^{\frac{1}{2}} \quad \text{i.e.,}$$

$$F(x) = \left[ 1 - \frac{b^*}{x^2} - \frac{4}{E^*} (x^{-12} - x^{-6}) \right]^{\frac{1}{2}}$$

As usual,  $F(R_0) = F(x_0) = 0$  defines the classical turning point  $R_0$  (or  $x_0$ ).  $E = \frac{1}{2} \mu v_0^2$  is the incident relative kinetic energy,  $E^* \equiv E/\epsilon$ ,  $b^* \equiv b/\sigma$  are the reduced energy and impact parameter, respectively, and  $\bar{V}(R)$  is the orientation-averaged potential (Eq. 9).

- 
9. Notation is that of A. R. Edmonds, "Angular Momentum in Quantum Mechanics", Princeton Univ. Press, Princeton, N.J. (1957), Chap. 2.
  10. See Ref. 8, Chap. 1 and Appendix.

Thus the reduced action may be expressed:

$$G(\theta, \phi) = \frac{4\epsilon\sigma}{\hbar v_0} \sum_{\ell=1}^3 \sum_m A_m^{(\ell)} C_m^{(\ell)*}(\theta, \phi), \quad (15)$$

where the  $A_m^{(\ell)}$  are given by the following relations:

$$\begin{aligned} A_0^{(0)} &= I_{00}^{(12)} - I_{00}^{(6)} \\ A_m^{(1)} &= b_1 I_{1m}^{(12)} - \frac{3c}{5} I_{1m}^{(7)} \\ A_m^{(2)} &= b_2 I_{2m}^{(12)} - a_2 I_{2m}^{(6)} \\ A_m^{(3)} &= -\frac{2c}{5} I_{3m}^{(7)} ; \end{aligned} \quad (16)$$

the twelve  $I_{lm}^{(n)}$  are integrals defined as follows:

$$I_{lm}^{(n)} \equiv 2 \int_{x_0}^{\infty} dx [x^n F(x)]^{-1} C_m^{(l)}(\theta', 0) = 2 b^{*(l-n)} \int_0^{\infty} dy \frac{y^{n-2}}{F(y)} C_m^{(l)}(\theta', 0) \quad (17)$$

where  $y \equiv b^*/x$ ,  $F(y) = \left[ 1 - y^2 - \frac{4}{E^*} \left( \frac{y^{12}}{b^{*12}} - \frac{y^6}{b^{*6}} \right) \right]^{1/2}$  and  $F(y_0) = 0$

The angle  $\theta'$  is itself a function of  $y$ , i.e., an integral over the trajectory (Eq. 21). It is noted that the integrals are functions of  $b^*$  and  $E^*$ , and are independent of the potential parameters.

$G(\theta, \phi)$  is re-written in a form more suitable for computation:

$$\begin{aligned}
 G(\theta, \phi) = \frac{4\pi}{\Lambda^* E^{*1/2}} & \left\{ B_1 + B_2 \cos \theta + B_3 \sin \theta \cos \phi + B_4 \cos \theta \sin \theta \cos \phi \right. \\
 & + B_5 \cos^2 \theta + B_6 \sin^2 \theta \cos^2 \phi + B_7 \cos^3 \theta \\
 & + B_8 \cos^2 \theta \sin \theta \cos \phi + B_9 \cos \theta \sin^2 \theta \cos^2 \phi \\
 & \left. + B_{10} \sin^3 \theta \cos^3 \phi \right\} \tag{18}
 \end{aligned}$$

where  $\Lambda^* \equiv h/\sigma(2\mu\epsilon)^{1/2}$  is the "quantum parameter".

The  $B$  coefficients are functions of the integrals  $I_{lm}^{(n)}$  (and thus  $b^*$  and  $E^*$ ) and the anisotropy parameters:

$$B_1 = \left(1 - \frac{1}{2}b_2\right) I_{00}^{(12)} - \left(1 - \frac{1}{2}a_2\right) I_{00}^{(6)}$$

$$B_2 = b_1 I_{10}^{(12)}$$

$$B_3 = -\sqrt{2} b_1 I_{11}^{(12)}$$

$$B_4 = \sqrt{6} \left[ a_2 I_{21}^{(6)} - b_2 I_{21}^{(12)} \right]$$

$$B_5 = b_2 \left[ \frac{3}{2} I_{00}^{(12)} - \sqrt{6} I_{22}^{(12)} \right] - a_2 \left[ \frac{3}{2} I_{00}^{(6)} - \sqrt{6} I_{22}^{(6)} \right]$$

$$B_6 = \sqrt{6} \left[ b_2 I_{22}^{(12)} - a_2 I_{22}^{(6)} \right]$$

$$B_7 = c \left[ 2\sqrt{\frac{2}{15}} I_{32}^{(7)} - I_{10}^{(7)} \right]$$

$$B_8 = 3c \left[ \sqrt{2} I_{11}^{(7)} - \frac{4}{\sqrt{5}} I_{33}^{(7)} \right]$$

$$B_9 = -2\sqrt{\frac{6}{5}} c I_{32}^{(7)}$$

$$B_{10} = \frac{4}{\sqrt{5}} c I_{33}^{(7)}$$

(19)

The integrals which were actually computed differ slightly from the  $I_{lm}^{(n)}$  by simple numerical factors; they are defined

$$I_{(n,p,q)} = 2 b^{*(l-n)} \int_0^{y_0} dy \cdot \frac{y^{n-2}}{F(y)} \cdot \cos^p[\theta'(y)] \cdot \sin^q[\theta'(y)] \quad (20)$$

where

$$\theta'(y) = \int_0^y dy/F(y) \quad (21)$$

such that the classical deflection angle  $\chi^{10}$  is given by

$$\chi = \pi - 2\theta'(y_0) \quad (22)$$

The conversion factors relating  $I_{(n,p,q)}$  to  $I_{lm}^{(n)}$  are given in Appendix I. 11

In the limit of large  $b^*$  and  $E^*$  (the region of validity of the "straight-line" approximation used in I), these integrals become independent of  $E^*$  and can be evaluated analytically. These asymptotic forms (listed in Appendix I) have proven useful in checking the computed integrals and in considering the problem of selection rules.

- - - - -  
11. These integrals may be of interest in connection with pressure-broadening theory. For early work, see P. W. Anderson, Phys. Rev. 76, 647 (1949); 80, 511 (1950); M. Baranger, ibid., 111, 481, 494 (1958); more recently, e.g., see Krishnaji and S. L. Srivastava, J. Chem. Phys. 42, 1546 (1965).

#### 4. Matrix Elements and Transition Probabilities

As in I, the matrix elements and transition probabilities are evaluated by direct numerical integration. To this end, Eq. 8 is put into the form:

$$P(j'm'jm|b,E) \equiv P_{\beta\alpha}(b^*, E^*) = X^2 + Y^2 \quad (23)$$

where

$$\begin{cases} X \\ Y \end{cases} = \int_0^{2\pi} \int_0^\pi d\theta d\phi \sin\theta \cdot f_{\beta\alpha}(\theta) \cdot \begin{cases} \cos [G(\theta, \phi) + (m'-m)\phi] \\ \sin [G(\theta, \phi) + (m'-m)\phi] \end{cases}$$

The angular functions  $f_{\beta\alpha}(\theta)$  (obtained directly by consideration of a table of spherical harmonics) are listed, for reference, in Appendix II. A brief outline of the quadrature technique is presented in Appendix III. Note that

$$P(j'm'jm) = P(jmj'm') .$$

#### 5. Selection Rules

It is convenient first to consider an idealized experimental situation in which the polar diatomic (target) molecules are essentially at rest in a homogeneous electric field  $\mathbf{E}$  (which establishes the axis of space quantization). The beam of (projectile) atoms (of mass equal to the reduced mass of the atom-molecule system) is directed with the velocity  $v_0$  along the field axis (the z-axis); i.e., Fig. 1 of I. It is desired to develop the selection rules for  $j,m \rightarrow j',m'$  transitions which apply under these circumstances.

To this end it is instructive to expand the exponential in Eq. 8. Successive terms in the resulting development for  $P_{\text{ex}}$  are then examined. The first term yields directly the familiar result of first-order time-dependent perturbation theory.

In the limiting case (that dealt with in I) of a straight line trajectory along  $z$ , all action integrals  $I_{lm}^{(n)}$  vanish except those for which  $|l+|m|$  is even (by symmetry of the  $C_m^{(l)}(\theta, \phi)$ ).

Thus what remains is the matrix element of the sum

$$\begin{aligned} & \langle j'm' | \sum_{l=1}^3 \sum_m A_m^{(l)} C_m^{(l)*}(\theta, \phi) | jm \rangle \\ &= \sum_{l=1}^3 \sum_m A_m^{(l)} \langle j'm' | C_m^{(l)*}(\theta, \phi) | jm \rangle \end{aligned} \quad (24)$$

Noting that  $\langle j_1 j_2 j_3 | C_{j_1 j_2 j_3}^{(l)} \rangle$  vanishes unless  $j_1 + j_2 + j_3$  is even, the selection rules for this case become:

$ \Delta j $	$ \Delta m $
1	1
2	0, 2
3	1, 3

Taking into account higher order terms in the expansion, one obtains "harmonics", i.e.

<u><math> \Delta_j </math></u>	<u><math> \Delta_m </math></u>	
even	even	
odd	odd	
		rule 1 - "parallel" configuration

with odd-even combinations forbidden.

However, in another type of experimental arrangement the projectile beam ( $\underline{\nu}_0$ ) could be directed perpendicular to the orientation axis ( $\underline{E}$ ). Using the same arguments as above one obtains the selection rules for the first order approximation:

<u><math> \Delta_j </math></u>	<u><math> \Delta_m </math></u>
1	0
2	0,2
3	0,2

Taking into account higher order terms, one finds

<u><math> \Delta_j </math></u>	<u><math> \Delta_m </math></u>	
even	even	
odd	even	
		rule 2 - "perpendicular" configuration

i.e., "odd" transitions in  $m$  are forbidden.

(For any intermediate angle between  $\underline{E}$  and  $\underline{\nu}_0$ , no "general" rule exists.)

Returning now to the first experimental arrangement, but taking cognizance of the non-linear trajectory, one expects the following behavior: for large  $b^*$ , selection rule 1 should dominate, but as  $b^*$  is decreased and all the  $C_m^{(n)}$  become important no selection rule will be operative; collisions will populate all (energetically accessible) rotational states to a greater or lesser extent.

In order to deal with an actual experimental arrangement, one must take into account the finite velocity and mass of the molecules and the atoms, and the possibility of an arbitrary angle between the beam direction and the orientation axis. One may rotate either the  $C_m^{(n)}(\theta, \phi)$  or the eigenfunctions of the rotor in the direction of the relative velocity vector. With the aid of the action integrals now evaluated (which represent a complete set for the intermolecular potential considered) either procedure can be carried out.

#### 6. Inelastic Total Cross Sections.

The total cross section  $\sigma_{\beta\alpha}$  for the  $\alpha \rightarrow \beta$  transition is given semiclassically by the integral

$$\sigma_{\beta\alpha}(E) = 2\pi \int_0^\infty b P_{\beta\alpha}(b, E) db \quad (25)$$

so that the "reduced" cross section is simply

$$\sigma_{\beta\alpha}^*(E^*) \equiv \sigma_{\beta\alpha} / \pi \sigma^2 = 2 \int_0^\infty b^* P_{\beta\alpha}(b^*, E^*) db^* \quad (26)$$

Thus  $\sigma_{\beta\alpha}^*$  is readily evaluated by integrating plots of partial total cross sections  $b^* P(b^*)$  vs.  $b^*$  (analogous to Fig. 3 of I).

It is also of interest to obtain the total inelastic total cross section from state  $\alpha$ , i.e., the quantity

$$\begin{aligned}\sigma_{inel,\alpha}^* &= \sum_{\beta(\neq\alpha)} \sigma_{\beta\alpha}^* = 2 \int_0^\infty b^* P_{inel,\alpha}(b^*, E^*) db^* \\ &= \int_0^\infty P_{inel,\alpha}(b^*, E^*) db^{*2} \quad (27)\end{aligned}$$

where

$$P_{inel,\alpha} = \sum_{\beta(\neq\alpha)} P_{\beta\alpha}$$

is the total inelastic transition probability.

## 7. Parameters

At the present time, it is difficult to find a system (atom-polar diatomic molecule) for which a meaningful theoretical (or even semi-empirical) estimate of both the short- and long-range anisotropic interaction is available.<sup>12</sup> It would therefore, be futile at this stage to attempt a detailed computation of rotational transition probabilities and cross sections for some specific system with the

12. Recently, H. G. Bennewitz (private communication) has carried out certain elastic scattering experiments involving polarized beams of TlF which have bearing on the repulsive anisotropy. Earlier work by H. G. Bennewitz, K. H. Kramer, W. Paul and J. P. Toennies [Z. Physik. 177, 84 (1964)] has led to a fairly reliable value of the  $a_2$  coefficient for TlF - rare gas.

expectation that numerical results could be compared with (eventual) experiment. Rather, it appears more reasonable to (1) explore the dependence of the calculated transition probabilities upon the various reduced "internal" parameters ( $\Lambda^*$ ,  $a_2$ ,  $b_1$ ,  $b_2$ ,  $c$ ) which characterize the interaction, hoping to establish the main causal relationships (and allow the possibility of future interpolation) and (2) study the dependence upon the reduced "external" parameters ( $b^*$ ,  $E^*$ ) characterizing the collision, for a few selected sets of internal parameters. In this connection the following arbitrary choices have been made:

Set 1: Homonuclear diatomic; long-range anisotropy only (corresponding to a case considered in I, but with full trajectory and action treatment):  $\Lambda^* = 7.4022$ ,  $a_2 = 0.28527$ ,  $b_1 = b_2 = c = 0$ .

Set 2: As in Set 1, but with  $\Lambda^* = 0.1$ ,  $a_2 = 0.3$ ,  $b_1 = b_2 = c = 0$ .

Set 3: Homonuclear diatomic; both long- and short-range interactions:

$$\Lambda^* = 0.1, a_2 = 0.3, b_2 = 0.5, b_1 = c = 0.$$

Set 4: Heteronuclear diatomic, long-range anisotropies only:

$$\Lambda^* = 0.1, a_2 = 0.3, b_1 = b_2 = 0, c = 2.$$

Set 5: Heteronuclear diatomic; both long- and short-range interactions,

but negligible  $R^{-7} \cos^3\theta$  term (i.e.,  $\alpha \mu Q \approx 0$ ):

$$\Lambda^* = 0.1, a_2 = 0.3, b_1 = b_2 = 0.5, c = 0.$$

Set 6: Heteronuclear polar diatomic. As in Set 5, but with

appreciable  $R^{-7}$  term:  $\Lambda^* = 0.1, a_2 = 0.3, b_1 = b_2 = 0.5,$   
 $c = 2.$

(Intended to approximate the system TiF-Ar.)

## 8. Results

### A. Action Integrals.

Tables AIV 1-12 (Appendix IV) summarize the results of the computations of the action integrals  $I(n,p,q)$  as a function of  $b^*$  (from 0.01 to 5) and  $E^*$  (from 1 to 100): Tables AIV 13 and 14 list ancillary results, i.e., reduced reciprocal turning points ( $y_0$ ) and deflection angles ( $\chi$ ), which are found to accord well with the literature<sup>10</sup>.

The integrals are plotted in Figs. 1-3, which show the dependence of  $I(6,p,q)$ ,  $I(7,p,q)$  and  $I(12,p,q)$  upon  $b^*$  at  $E^* = 10$ , and in Figs. 4-6, which show something of the energy dependence of the twelve integrals  $I(n,p,q)$ .

Having the full set of  $I(n,p,q)$  as a function of  $b^*$  and  $E^*$  available (once and for all) on punched cards, they could be readily combined with any of various sets of anisotropy parameters to yield (for a chosen  $b^*$  and  $E^*$ ) a set of B constants (Eq. 9). Then, upon selection of  $\chi^*, G(\theta, \phi)$  is completely determined (Eq. 18).

### B. Transition Probabilities.

Appendix V summarizes the computed transition probabilities: Table AV 1 lists values for transitions involving the 0,0 state (i.e.,  $0,0 \rightarrow 0,0; 1,0; 1,\pm 1; 2,0; 2,\pm 1; 2,\pm 2; 3,0$ ; and  $4,0$ ), while Table AV 2 gives results for the 1,0 state (i.e.  $1,0 \rightarrow 1,0; 1,\pm 1; 2,0; 2,\pm 1; 2,\pm 2$ ; and  $3,0$ ).

The quadratures for the transition probabilities are believed to be numerically accurate in all cases, to better than  $\pm 0.001$ ; for any given entry the penultimate digit listed can be considered accurate. By way of confirmation, it is noted that for a large number of cases the sum of the computed transition probabilities (even for the limited number of transitions considered) totals as much as 0.999; yet in no case does it exceed unity.

For later reference, attention is directed to the important "null-" or "pseudo-elastic-transitions", i.e.,  $0,0 \rightarrow 0,0$  and  $1,0 \rightarrow 1,0$ , which serve as a monitor of the total inelastic component. The sum of the inelastic transition probabilities from state  $\alpha$  is given by

$$P_{inel,\alpha} = \sum_{\beta} P_{\beta\alpha} = 1 - P_{\alpha\alpha} . \quad (28)$$

Thus, even when the number of  $j'm'$  states considered in the computation is inadequate, the true sum of all the inelastic transition probabilities ( $\alpha \rightarrow \text{all } \beta$ ) may be found directly from the single computation  $P_{\alpha\alpha}$ .

Figs. 7-9 illustrate the dependence of the various transition probabilities  $P_{\beta\alpha}$  upon each of the "internal" parameters  $\Delta^*$ ,  $a_2$ ,  $b_1$ ,  $b_2$  and  $c$  at stated  $E^*$  and  $b^*$ ; Figs. 10-12 summarize the dependence of  $P_{\beta\alpha}$  upon  $b^{*2}$  for various parameter sets, while Figs. 13-14 show the results for  $P_{inel,\alpha}$ . In each of the latter figures the vertical line (for  $P_{inel,\alpha} = P_{\alpha\alpha} = \frac{1}{2}$ ) defines an important value of  $b^{*2}$ , designated  $S_{inel,\alpha}^*$ .

### C. Inelastic Total Cross Sections

Figs. 15-18 show the partial total cross sections, i.e.,

13. On the basis of extensive checking with different sets of integration intervals for widely different integrand cases.

plots of  $b^* \cdot P_{\beta\alpha}(b^*)$  vs.  $b^*$ , for certain parameter sets; these are, of course, closely related to the inelastic angular distribution functions. Results of graphical integrations of these plots (viz. Eq. 26) are presented in Table 1, which lists various reduced inelastic total cross sections  $\frac{14}{14} / \sigma_{\beta\alpha}^*$  at  $E^* = 1$  and 10.

Figs. 19 and 20 are plots of  $P_{\text{inel},\alpha}$  vs.  $b^{*2}$  at several values of  $E^*$ , for parameter Set 6. The areas under these curves (and those of Figs. 13 and 14) yield directly the total inelastic total cross section  $\sigma_{\text{inel},\alpha}^*$  (via Eq. 27); these and results for other parameter sets are tabulated together with the values of  $S_{\text{inel},\alpha}^*$  in Table 2. For obvious reasons  $S_{\text{inel}}^*$  is a good approximation to  $\sigma_{\text{inel}}^*$ .

The energy dependence of  $\sigma_{\text{inel},\alpha}^*$  (parameter set 6) is shown graphically in Fig. 21. Table 3 lists correspondingly the inelastic fraction of the total scattering cross section,  $\sigma_{\text{inel},\alpha}^* / \sigma_{\text{tot}}^*$ , vs.  $E^*$ .

## 9. Discussion

### A. Action Integrals

The general behavior of the action integrals  $I(n,p,q)$  (Figs. 1-6) is in accord with expectation. However, the substantial magnitudes of the five integrals which involve odd powers of  $\cos \theta'$  (and therefore vanish in the straight-line trajectory approximation) even at relatively large  $b^*$  should be noted. Thus, as a consequence of the curved trajectories, odd  $\Delta m$  transitions are allowed, even when the potential involves only anisotropies of even parity (e.g., Sets 1-3); this is in contrast to the results of the straight-line approximation (cf. I).

14. These results are, of course, somewhat too small due to the neglect of the contribution from low impact parameters.

### B. Transition Probabilities and Selection Rules

From the parameter-variation studies a number of plausible inferences may be drawn. At large  $b^*$  the long-range anisotropy parameters  $c$  and  $a_2$  dominate; as  $b^*$  is decreased the repulsive anisotropies  $b_1$  and  $b_2$  become important. The sign of  $b_2$  plays a significant role (at small  $b^*$ ) due to "destructive interference" with the  $a_2$  term. Of all the anisotropies, that associated with the Anderson dipole-quadrupole term ( $R^{-7} \cos^3 \theta$ ) exerts the greatest influence upon the total inelasticity, in accord with the findings of Toennies<sup>V</sup>. Of course, the smaller the value of the quantum parameter  $\lambda^*$ , i.e., the more "classical" the system, the more inelasticity (all other factors assumed constant).

For practical purposes there are no general selection rules; as  $b^*$  is decreased from large values successive inelastic transitions become important, reach a peak probability, then decrease in significance; upon entering the dominant-coupling<sup>3V</sup> region, the various transition probabilities approach a condition of randomness, as in I.

The sharp onset of "dominant-coupling" is illustrated in 13, 14, 19 and 20, Figs.<sup>X</sup>, which show the rapid, sigmoid "growth-curves" for  $P_{inel,\alpha}$  as  $b^{*2}$  is decreased. As  $b^{*2}$  becomes appreciably smaller than  $S_{inel,\alpha}^{*2}$  i.e.,  $b < (S_{inel,\alpha} / \pi)^{1/2}$  the randomness condition becomes apparent:  $\langle P_{\alpha\alpha} \rangle \cong \langle P_{\beta\alpha} \rangle = \frac{1}{N}$ , where  $N$  is the number of close-coupled  $(j,m;j'm')$  states.

From Tables 1 and 2 of Appendix V, it is seen that values of  $\langle P_{\beta\alpha} \rangle$  as small as  $10^{-3}$  are common at  $b^* \approx 1$ . Since

$N \cong 2 j'_{\max}^2$ , where  $j'_{\max}$  is the highest  $j'$  of the close-coupled group, this implies a  $j'_{\max} \approx 20$  (i.e., transitions with  $\Delta j \leq 20$  are of comparable probability<sup>15</sup>)

One may conclude<sup>13</sup> that the very complexity of the behavior of the transition probabilities in the rotational excitation problem is one of its principal virtues.

### C. Cross Sections

Inspection of Table 1 reveals a number of obvious regularities and inter-relationships in the behavior of the various inelastic cross sections for transitions from both 00 and 10 states.

The total inelastic total cross section is seen to be well approximated by  $S_{inel,\alpha}^*$ , where

$$S_{inel,\alpha}^* = b^{*2} (P_{\alpha\alpha} = \frac{1}{2}) , \quad (29)$$

and to be governed essentially by the long-range anisotropies (at least at moderate collision energies). With increasing  $E^*$  the repulsive anisotropies play a more significant role; however, it appears as though the details of the short-range interactions are of secondary importance in determining the total elasticity.

The results shown in Table 3 suggest that, although the inelastic cross section decreases with increasing  $E^*$ , the fractional inelastic contribution to the total scattering cross section is nearly independent of the collision energy.

### 10. Concluding Remarks

The present results have shown certain overall patterns of behavior for rotational excitation according to the sudden approximation. The question of the degree of validity of the approximation

15. However, the contribution to the total inelastic total cross section from any individual transition ( $j_m \rightarrow j'm'$ ) is small, and is dominated by the one small peak in its partial total cross section curve (i.e., angular distribution).

itself is left unanswered.<sup>16/</sup> However, it is expected that at moderate energies and for scattering angles  $\chi$  not too close to 0 or  $\pi$ , the qualitative picture, at least, has been correctly portrayed. Angular distributions of the various inelastic cross sections would be helpful in deducing the separate anisotropies; however, useful predictions of inelastic scattering cross sections for specific systems must await a fuller knowledge of the complete, anisotropic intermolecular potential function.

#### 11. Acknowledgments

The extensive coding of the computing programs was carried out most ably by Mrs. M. Taylor and Mrs. N. Gordon, assisted by Mrs. F. Greville, with valuable advice by Prof. S. E. Lovell. The computations were performed at the University of Wisconsin Computing Center using CDC 1604 and 3600 computers. The authors appreciate this essential contribution to the research. In addition thanks are due to Mr. R. Fenstermaker for assistance with the graphical integrations yielding the total cross sections.

- 
16. This question has been considered in some detail by J. L. J. Rosenfeld, manuscript in preparation (private communication, June, 1965). An alternate approximation scheme has been proposed by K. P. Lawley and J. Ross (J. Chem. Phys., in press).

TABLE I  
SUMMARY OF INELASTIC TOTAL CROSS SECTIONS

$\lambda^* = 0.1, \alpha_2 = 0.3$			Entries are $\sigma_{j'm}^*$ or $\sigma_{j'm}^*$	
			$j'm'$	$j'm'$
			10	11
E*	b <sub>1</sub>	b <sub>2</sub>	$\sigma_{inel,00}^*$	<.003
1	0	0	3.99	<.003
1	0.5	0.5	4.03	.010
1	0	0	5.08	.062
1	0.5	0.5	5.10	.080
10	0.5	0.5	3.31	.072

			$j'm'$	$j'm'$
			20	21
			22	2
E*	b <sub>1</sub>	b <sub>2</sub>	$\sigma_{inel,10}^*$	
1	0.5	0.5	0	3.65
1	0.5	0.5	2	4.60
10	0.5	0.5	2	2.96

TABLE 2.  
Total Inelastic Total Cross Sections

$$\Delta^* = 0.1, \quad a_2 = 0.3.$$

$E^*$	$b_1$	$b_2$	$c$	$jm$	$\sigma_{inel, jm}^*$	$s_{inel, jm}^*$
1	0	0	0	00	3.99	3.86
"	0.5	0.5	"	"	4.03	3.88
"	0	0	2	"	5.08	5.15
"	0.5	0.5	"	"	5.10	5.15
"	"	"	0	10	3.65	3.48
"	"	"	2	"	4.60	4.37
3	"	"	"	00	4.16	4.18
10	"	"	"	"	3.31	3.35
30	"	"	"	"	2.76	2.83
100	"	"	"	"	2.23	2.32
3	"	"	"	10	3.72	3.56
10	"	"	"	"	2.96	2.87
30	"	"	"	"	2.43	2.42
100	"	"	"	"	1.95	1.96

TABLE 3  
TOTAL SCATTERING CROSS SECTIONS

$E^*$	$\sigma_{tot}^* \nabla$	$\sigma_{inel,00}^*$	$\frac{\sigma_{inel,00}^*}{\sigma_{tot}^*}$	$\sigma_{inel,10}^*$	$\frac{\sigma_{inel,10}^*}{\sigma_{tot}^*}$
1	17.78	5.10	0.287	4.60	0.259
3	14.28	4.16	0.292	3.72	0.261
10	11.22	3.31	0.295	2.96	0.264
30	9.01	2.76	0.306	2.43	0.270
100	7.08	2.23	0.315	1.95	0.275

$\nabla$  For  $\nabla = 0.1$ , based on the equation:  $\sigma_{tot}^* = 7.081 \cdot (\nabla^* E^*)$ .

## LEGENDS FOR FIGURES

1. Dependence of action integrals  $I(6,p,q)$  upon the reduced impact parameter  $b^*$  at a reduced energy  $E^* = 10$ .
2. Action integrals  $I(7,p,q)$  vs.  $b^*$ , as in Fig. 1.
3. Action integrals  $I(12,p,q)$  vs.  $b^*$ , as in Figs. 1 and 2.
4. Energy dependence of action integrals  $I(6,p,q)$ . Computed points have been connected with straight lines.
5. Energy dependence of  $I(7,p,q)$ , as in Fig. 4.
6. Energy dependence of  $I(12,p,q)$ , as in Figs. 4 and 5.
7. Transition probabilities from the 00 state as a function of the quantum parameter,  $\Lambda^*$ , for the indicated values of the other parameters. The lower curve in each case is an expanded-scale presentation of the upper one. Computed points have been connected with straight lines.
8. Transition probabilities from the 00 state as a function of the long-range anisotropy parameters  $a_2$  and  $c$  for the indicated values of the other parameters; otherwise, as in Fig. 7.
9. Transition probabilities from the 00 state as a function of the short-range anisotropy parameters  $b_1$  and  $b_2$ ; otherwise, as in Figs. 7 and 8.
10. Transition probabilities from the 00 state as a function of the reduced impact parameter  $b^*$ ; otherwise, as in Figs. 7-9. Parameter sets 2 and 5 at  $E^* = 1$ .
11. Transition probabilities from the 00 state vs.  $b^*$  for parameter sets 4 and 6 at  $E^* = 1$ ; otherwise, as in Figs. 7-10.

## LEGENDS FOR FIGURES (cont'd)

12. Transition probabilities from the 10 state vs.  $b^*$  for parameter sets 5 and 6 at  $E^* = 1$ ; otherwise, as in Figs. 7-11.
13. Total inelastic transition probabilities from the 00 state,  $P_{inel,00}$ , as a function of  $b^{*2}$ , for parameter sets 2, 4, 5 and 6 at  $E^* = 1$ . The dashed vertical lines at  $P = \frac{1}{2}$  define the value of  $S_{inel}^*$  ( $\equiv b^{*2}$  at  $P = \frac{1}{2}$ ).
14. Total inelastic transition probabilities,  $P_{inel,10}$  from the 10 state as a function of  $b^{*2}$ , for parameter sets 5 and 6 at  $E^* = 1$ ; otherwise as in Fig. 13.
15. Plots of  $b^* P_{j'm'00}$  vs.  $b^*$  for parameter sets 2 and 5 at  $E^* = 1$ . From the areas under the various curves the inelastic total cross sections  $\sigma_{\beta\alpha}^*$  are obtained.
16. Plots of  $b^* P_{j'm'00}$  vs.  $b^*$  for parameter sets 4 and 6 at  $E^* = 1$ ; otherwise same as Fig. 15.
17. Plots of  $b^* P_{j'm'10}$  vs.  $b^*$  for parameter sets 5 and 6 at  $E^* = 1$ ; otherwise same as Figs. 15 and 16.
18. Plots of  $b^* P_{0000}$  vs.  $b^*$  for parameter sets 2,5; 4,6. Also  $b^* P_{1010}$  vs.  $b^*$  for parameter sets 5 and 6, all at  $E^* = 1$ .
19. Energy dependence of  $P_{inel,00}$  ( $b^{*2}$ ) for parameter set 6.
20. Energy dependence of  $P_{inel,10}$  ( $b^{*2}$ ) for parameter set 6.
21. Log-log plot of the energy dependence of the total inelastic total cross sections  $\sigma_{00}^*$  and  $\sigma_{10}^*$ . See also Table 3.

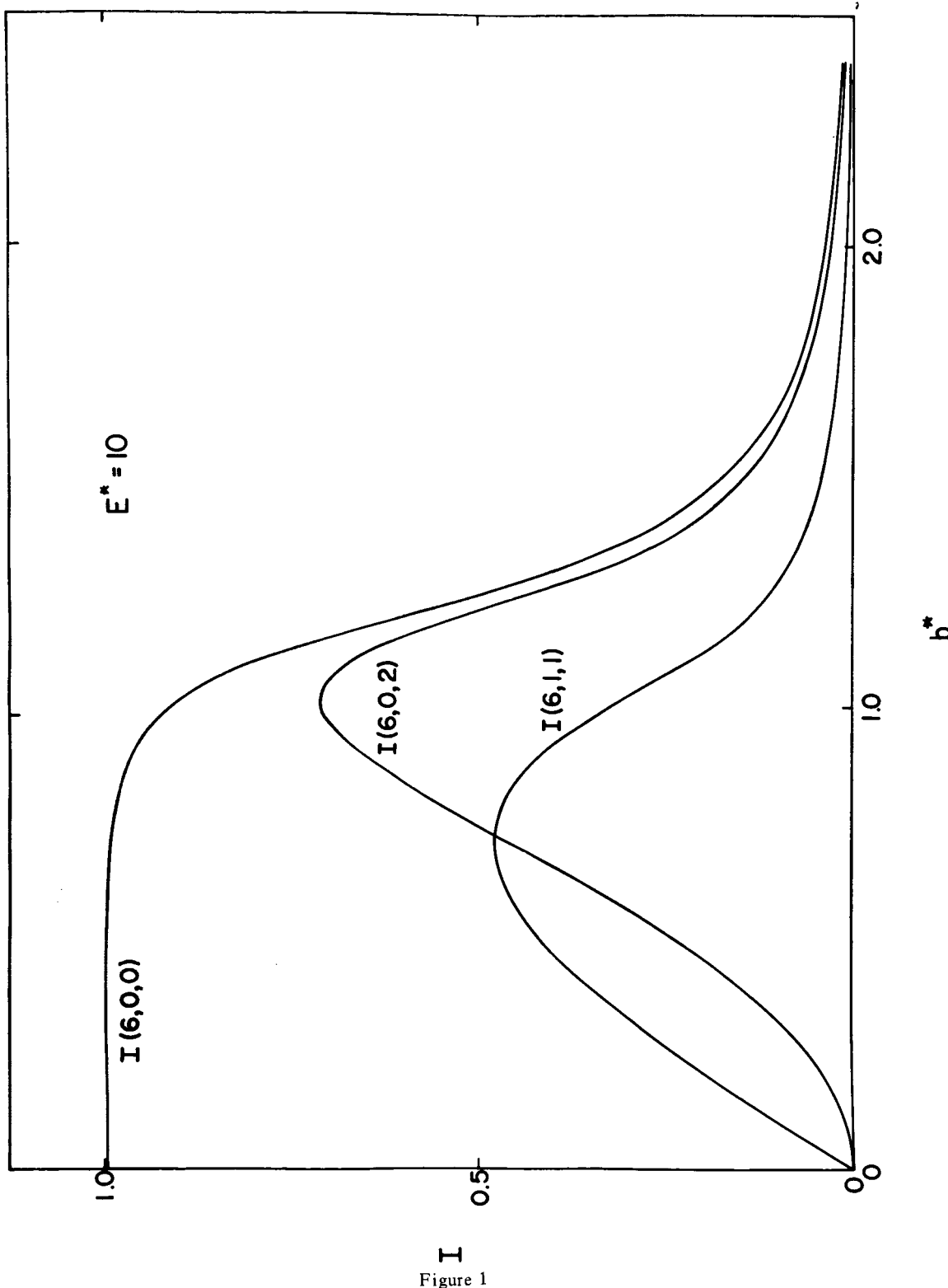


Figure 1

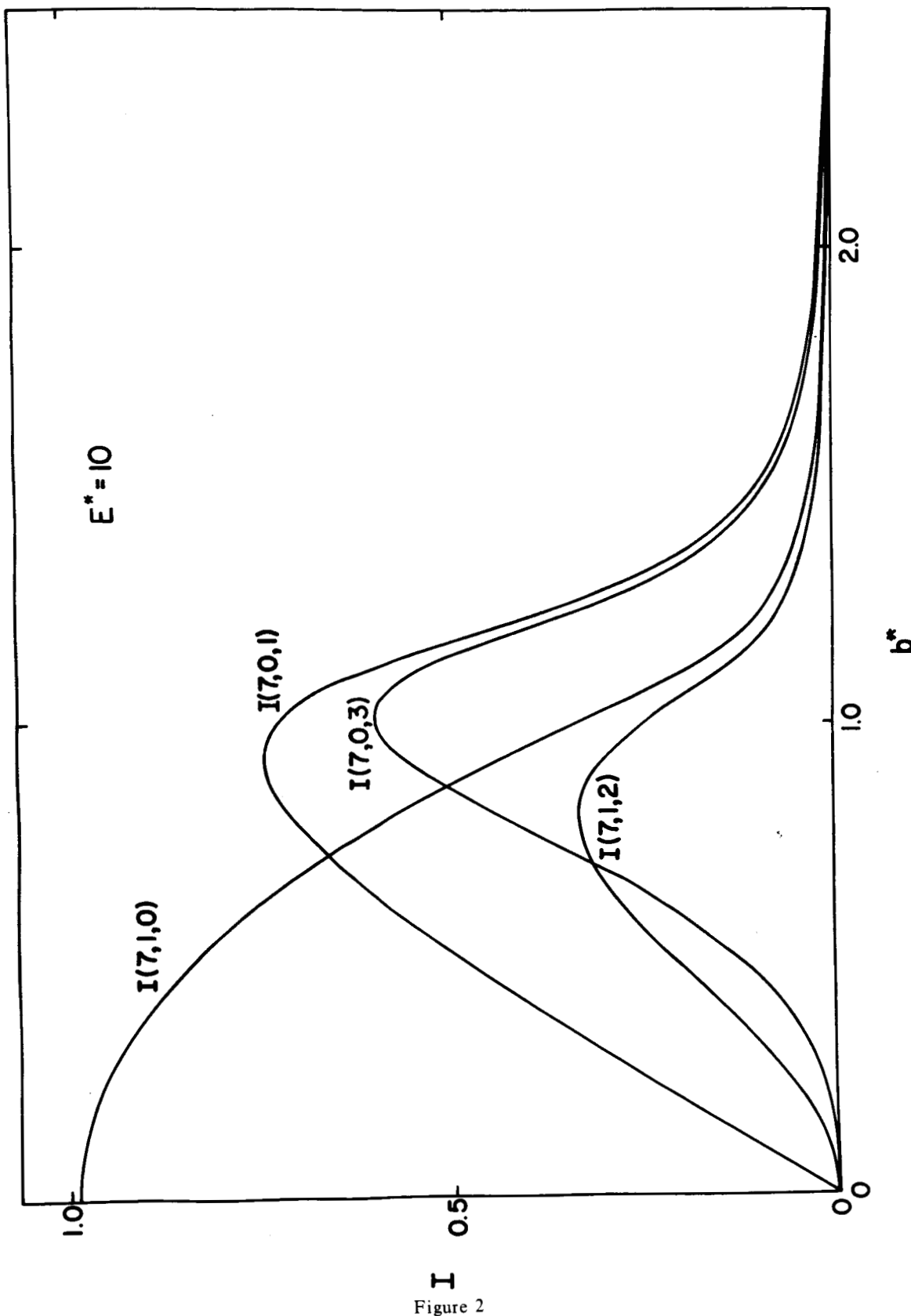


Figure 2

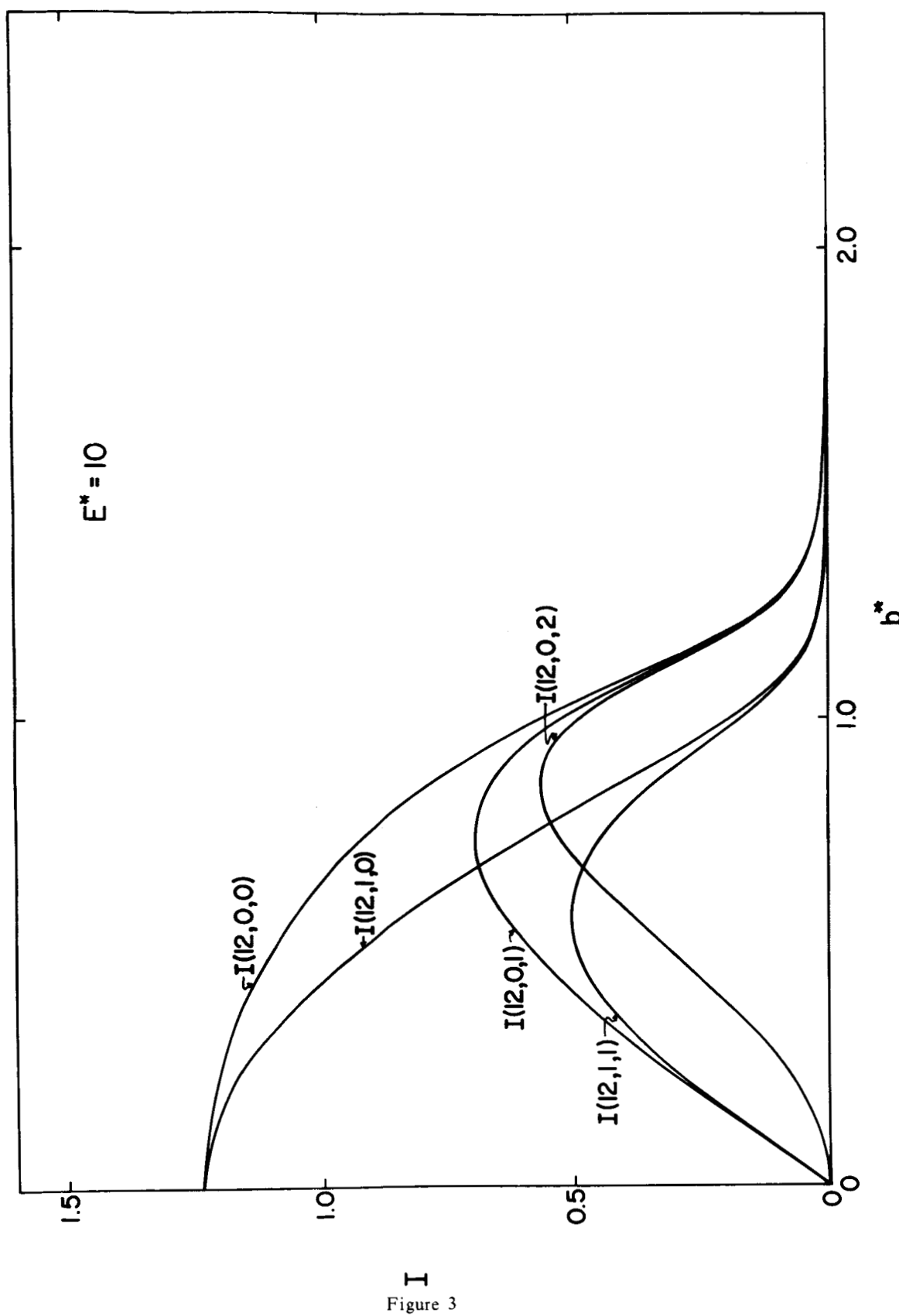


Figure 3

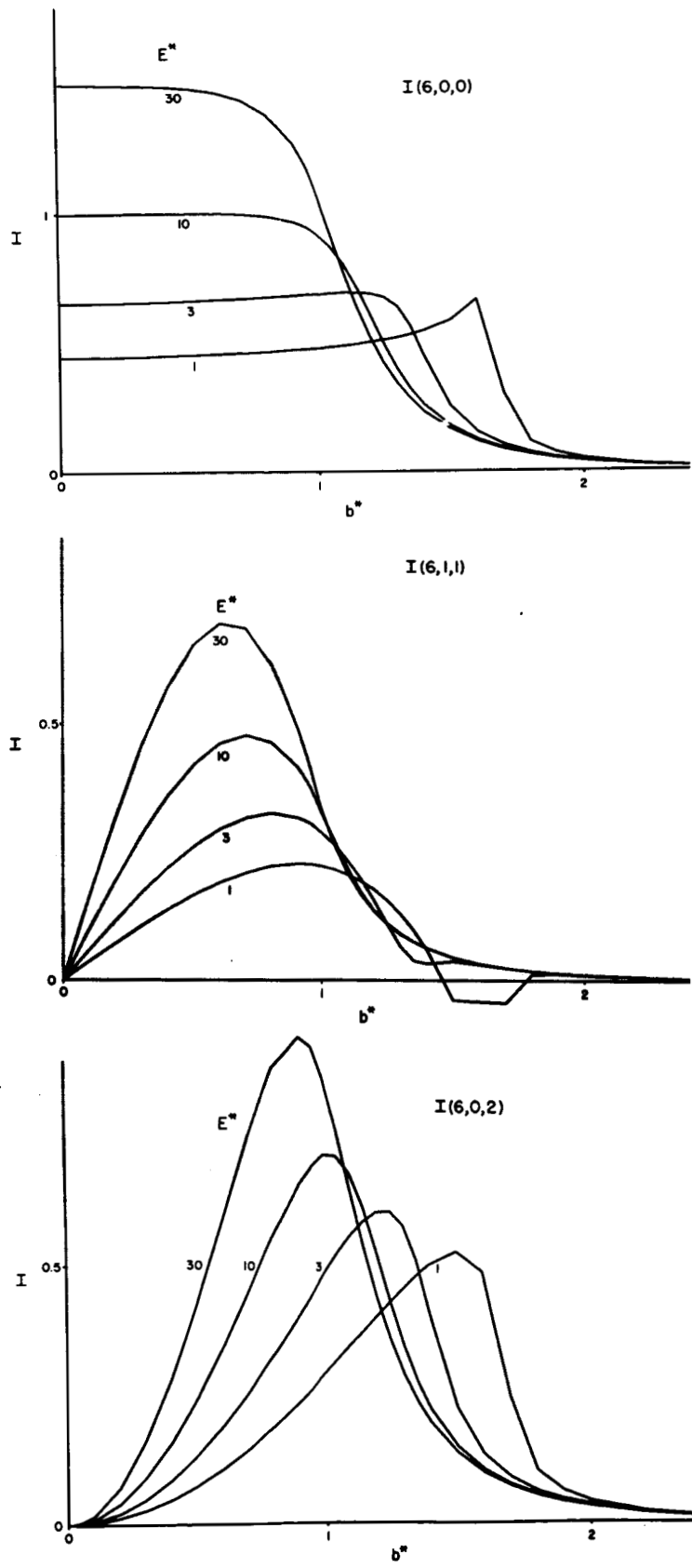


Figure 4

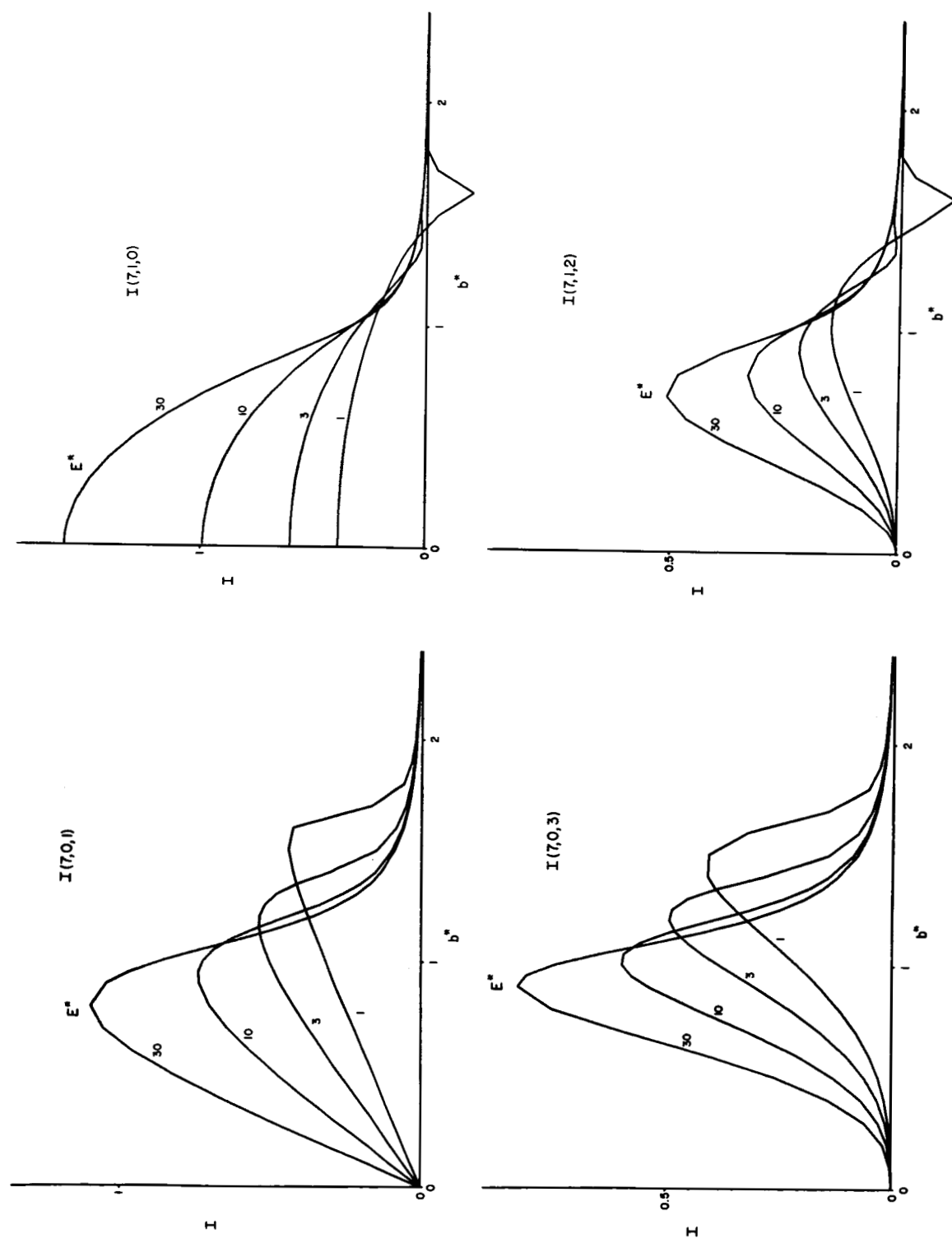


Figure 5

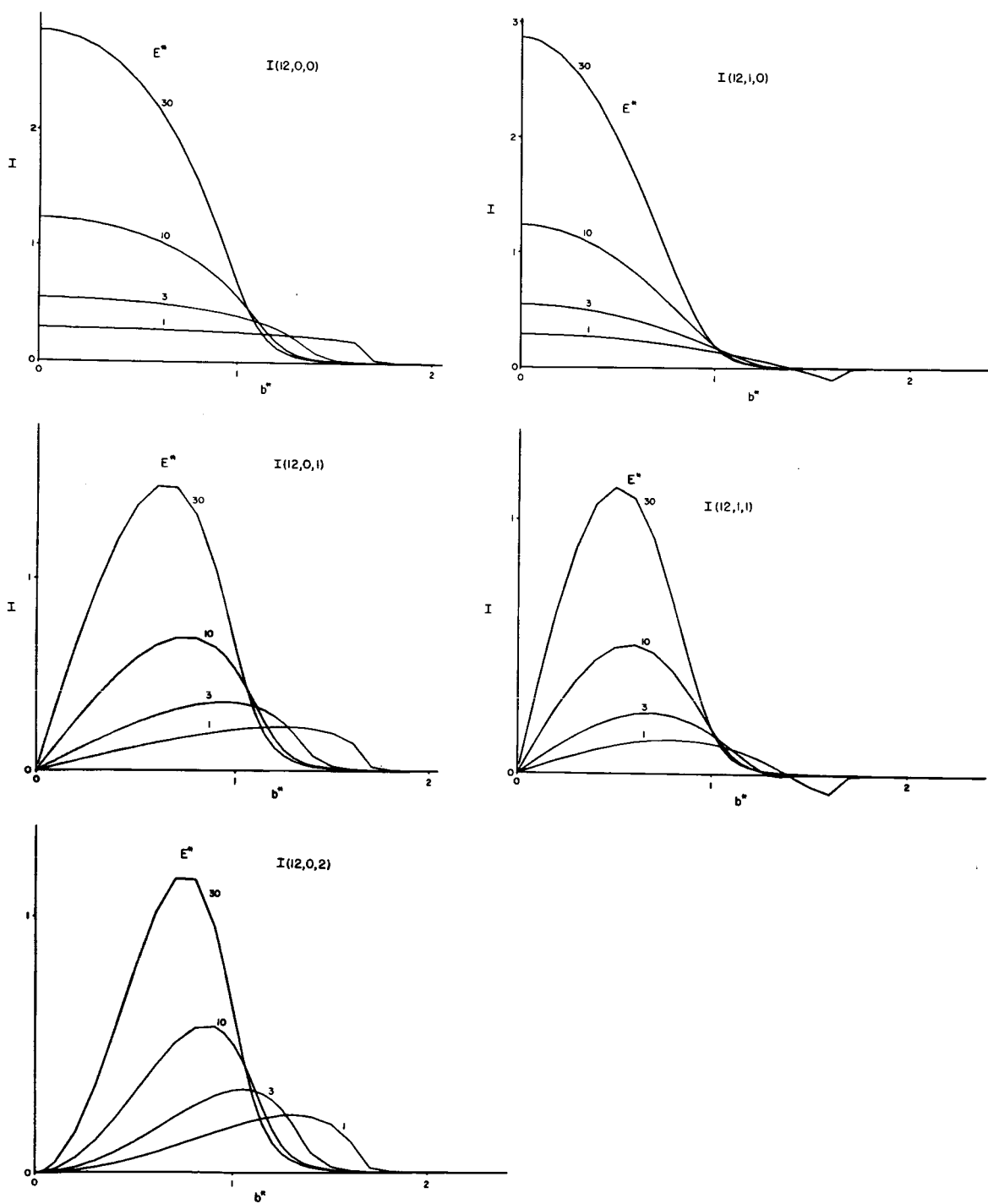


Figure 6

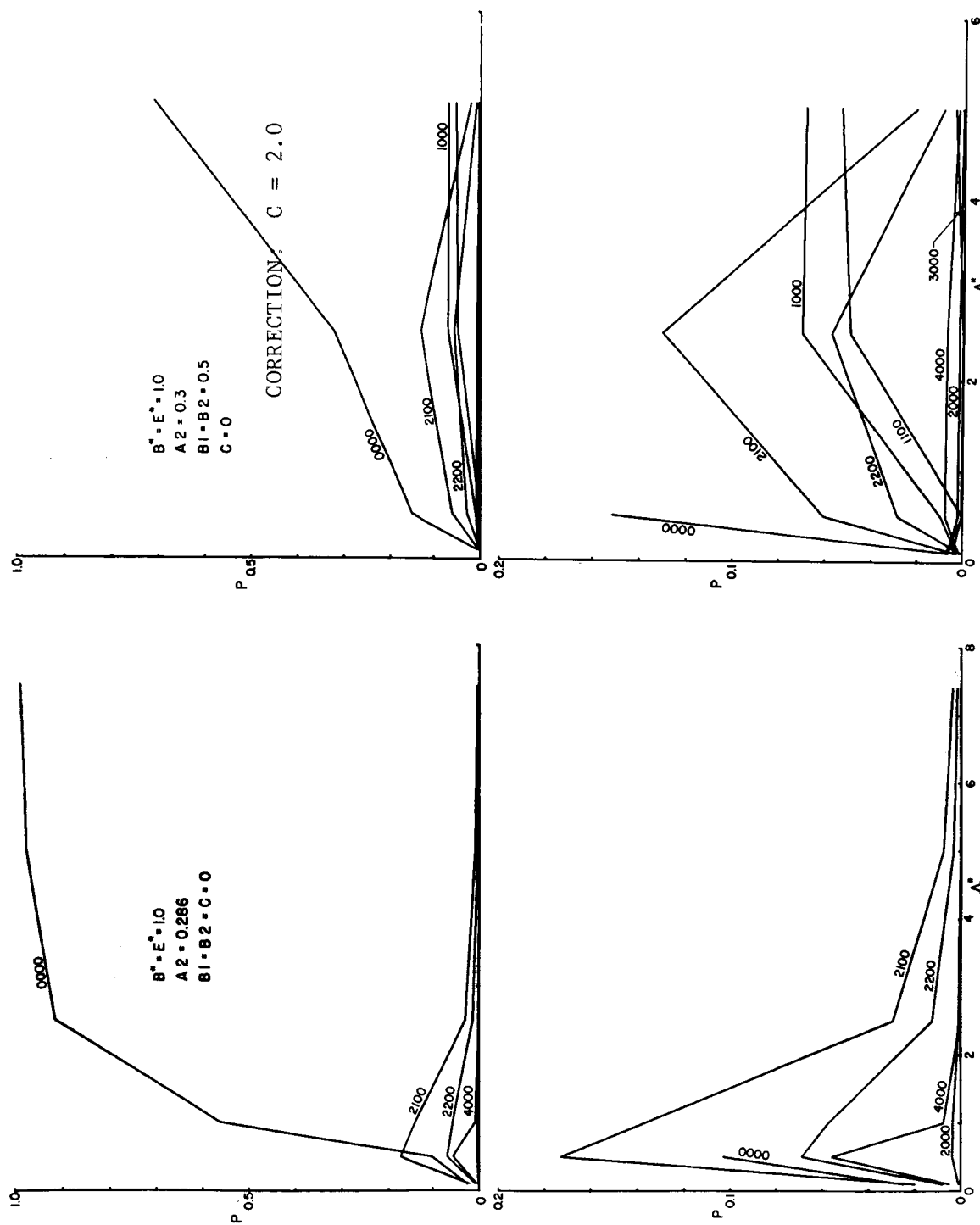


Figure 7

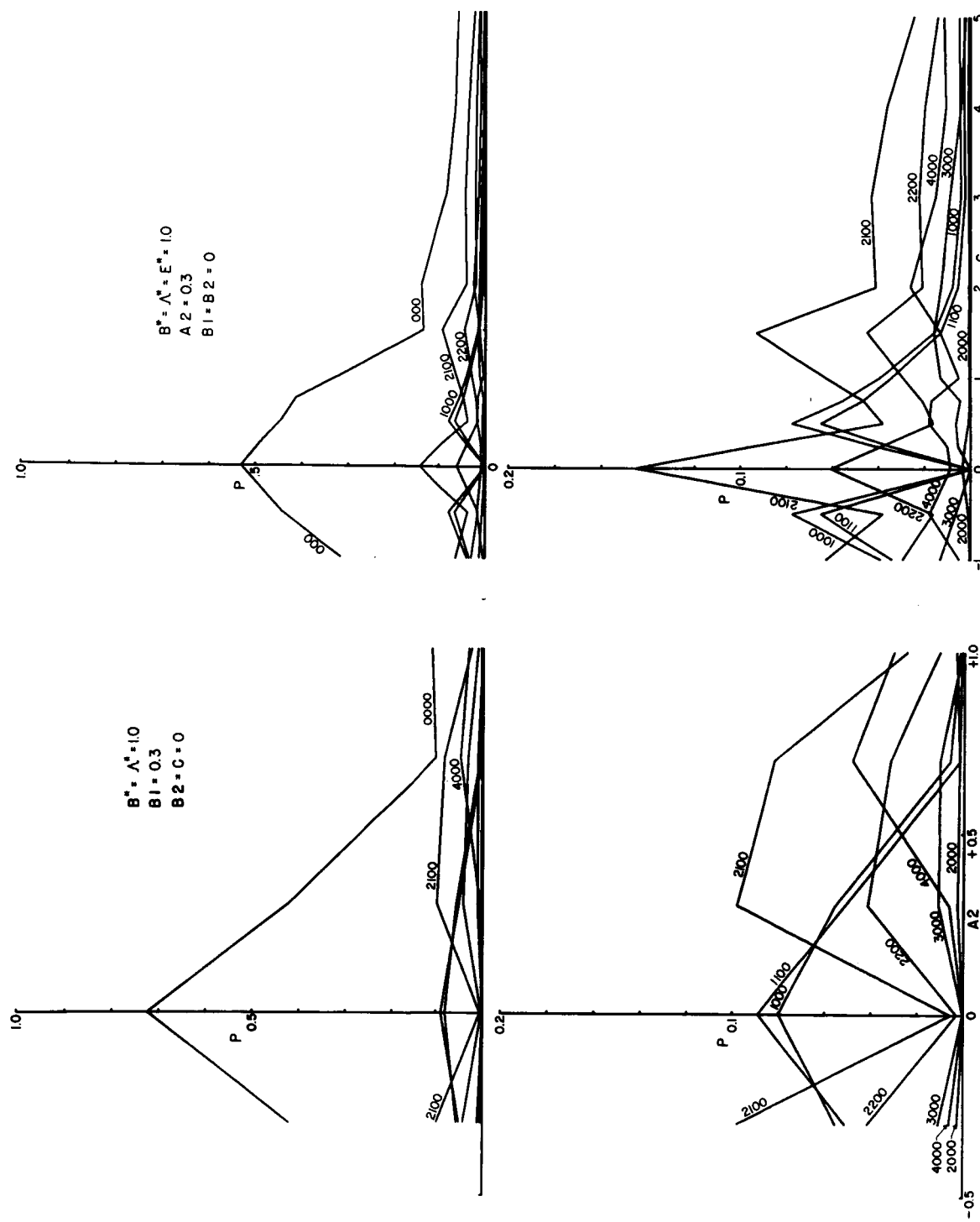


Figure 8

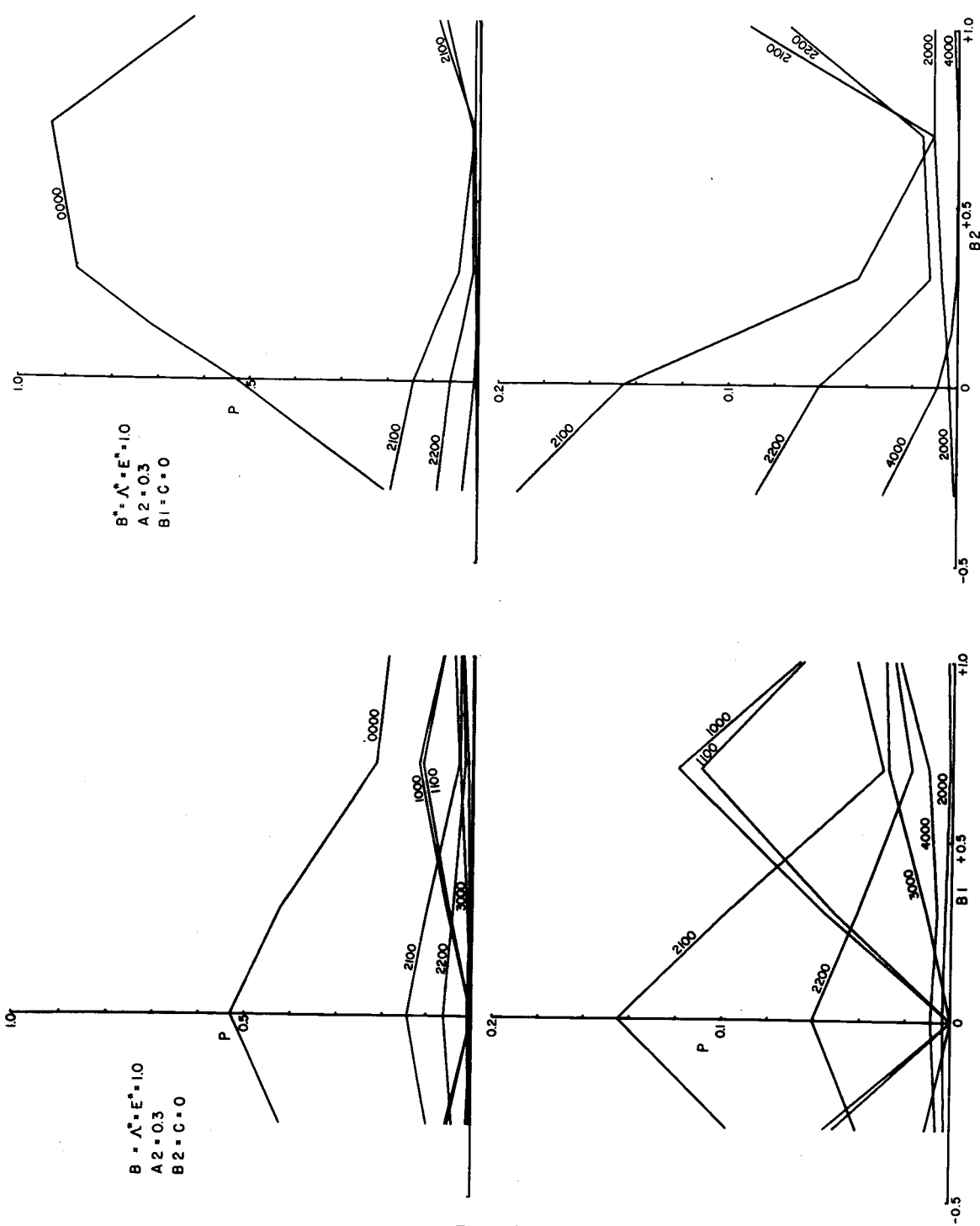


Figure 9

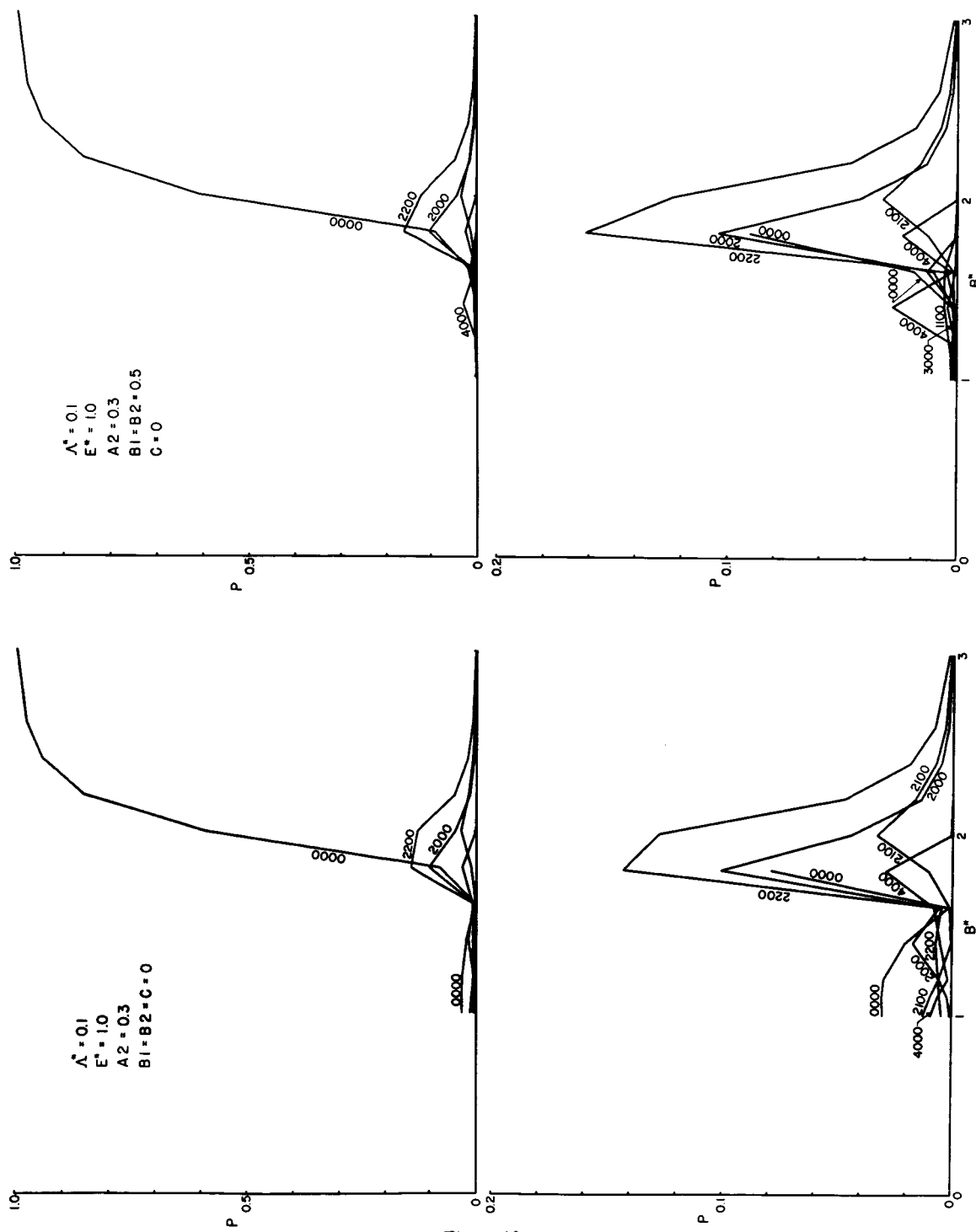


Figure 10

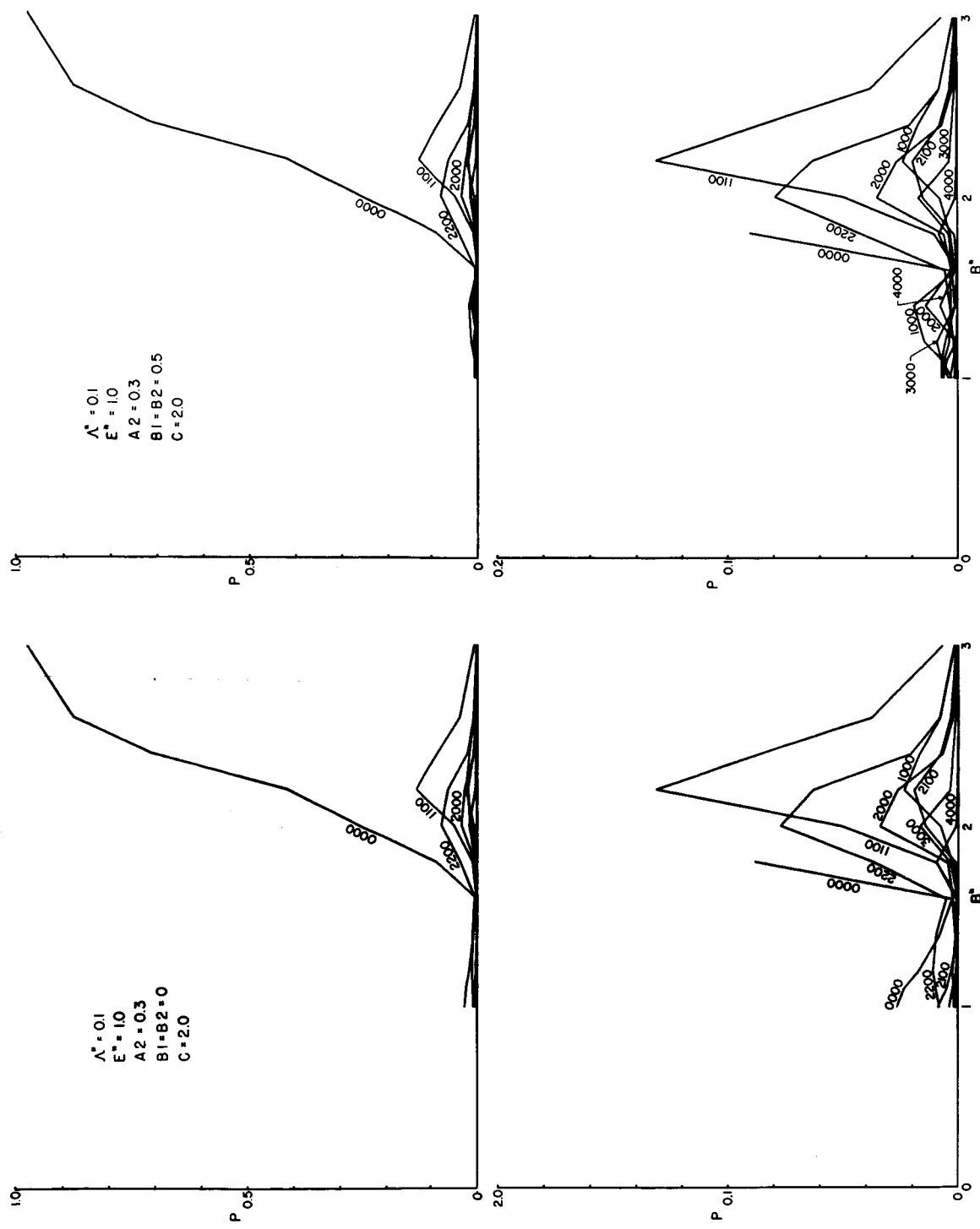


Figure 11

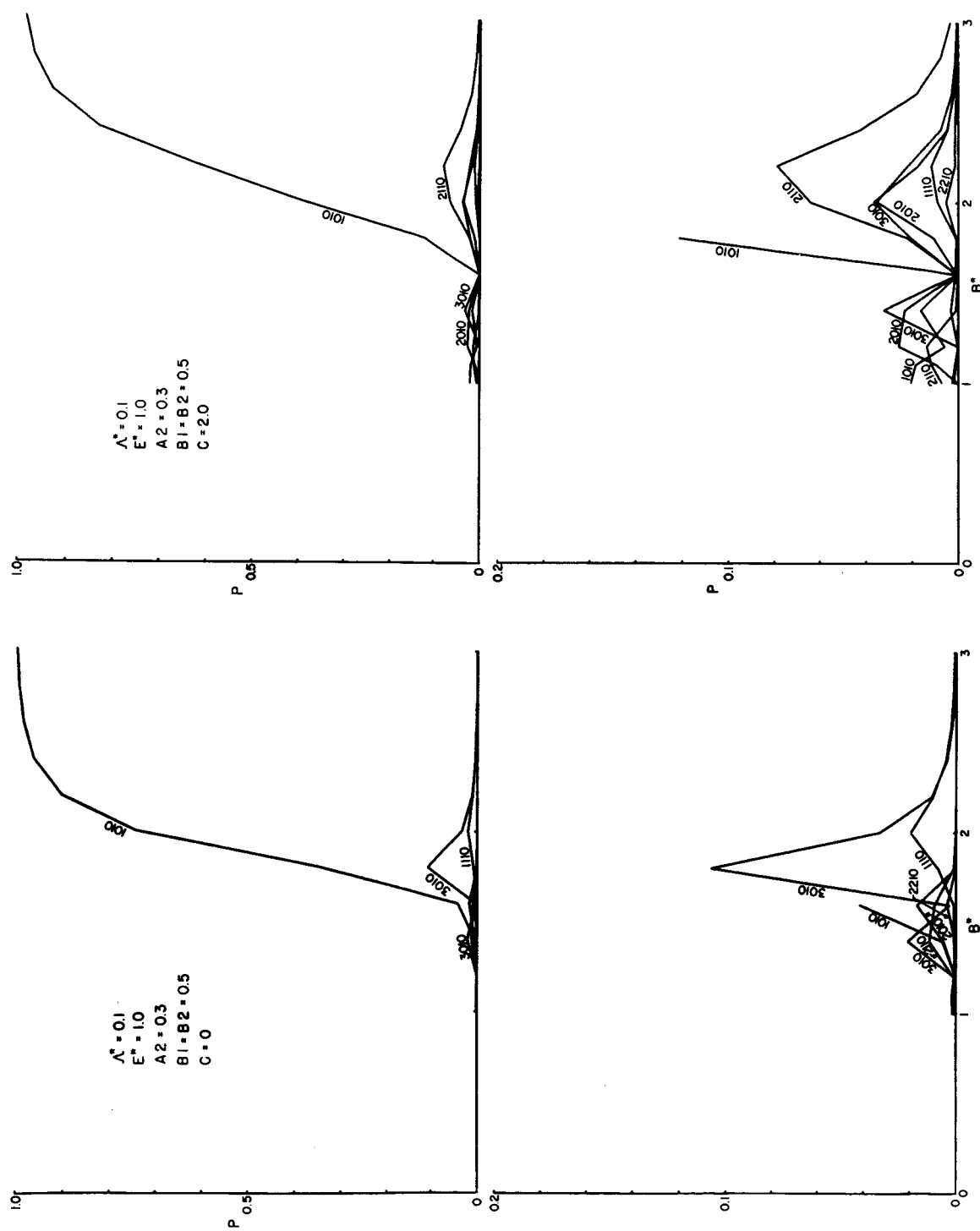


Figure 12

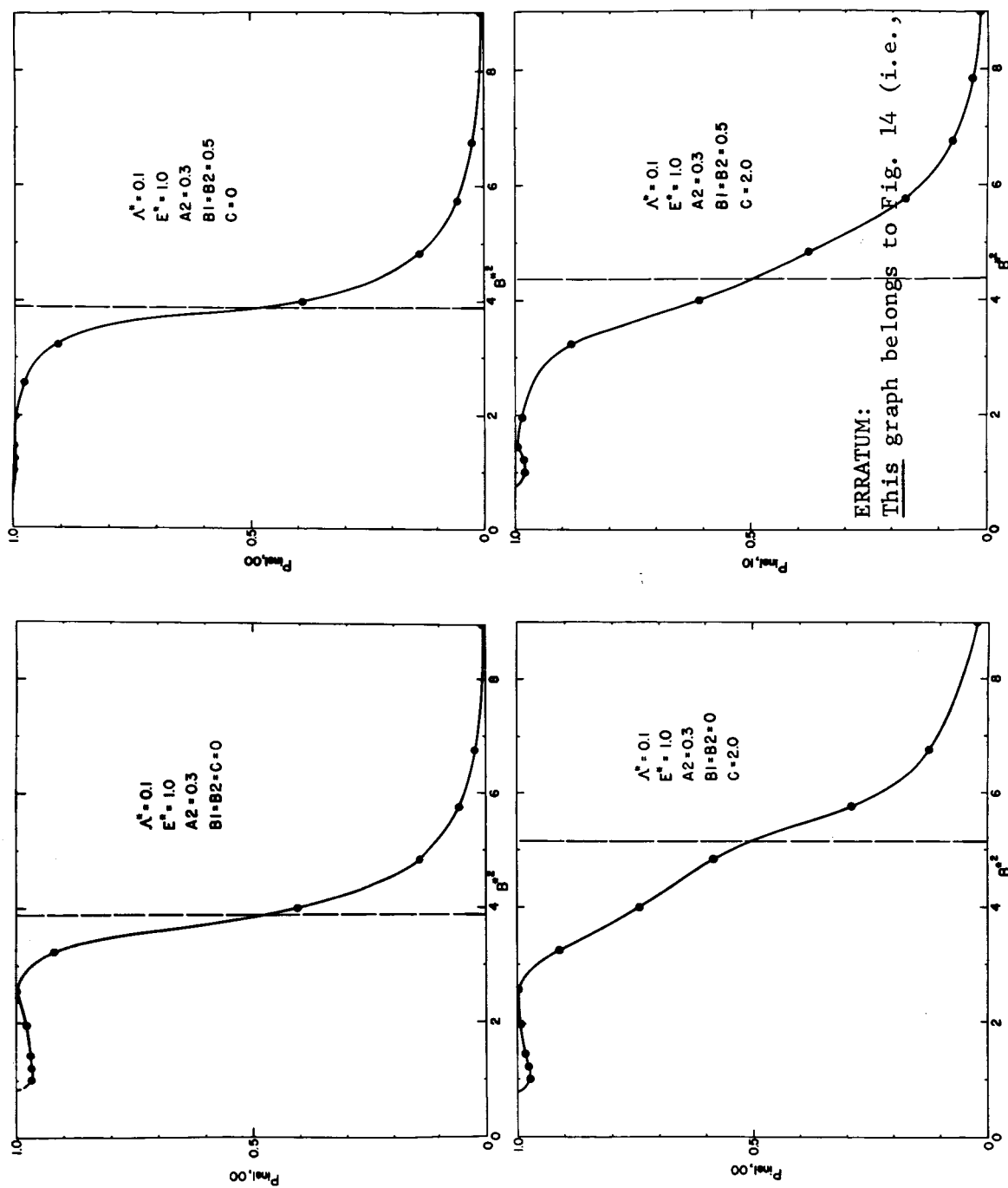


Figure 13

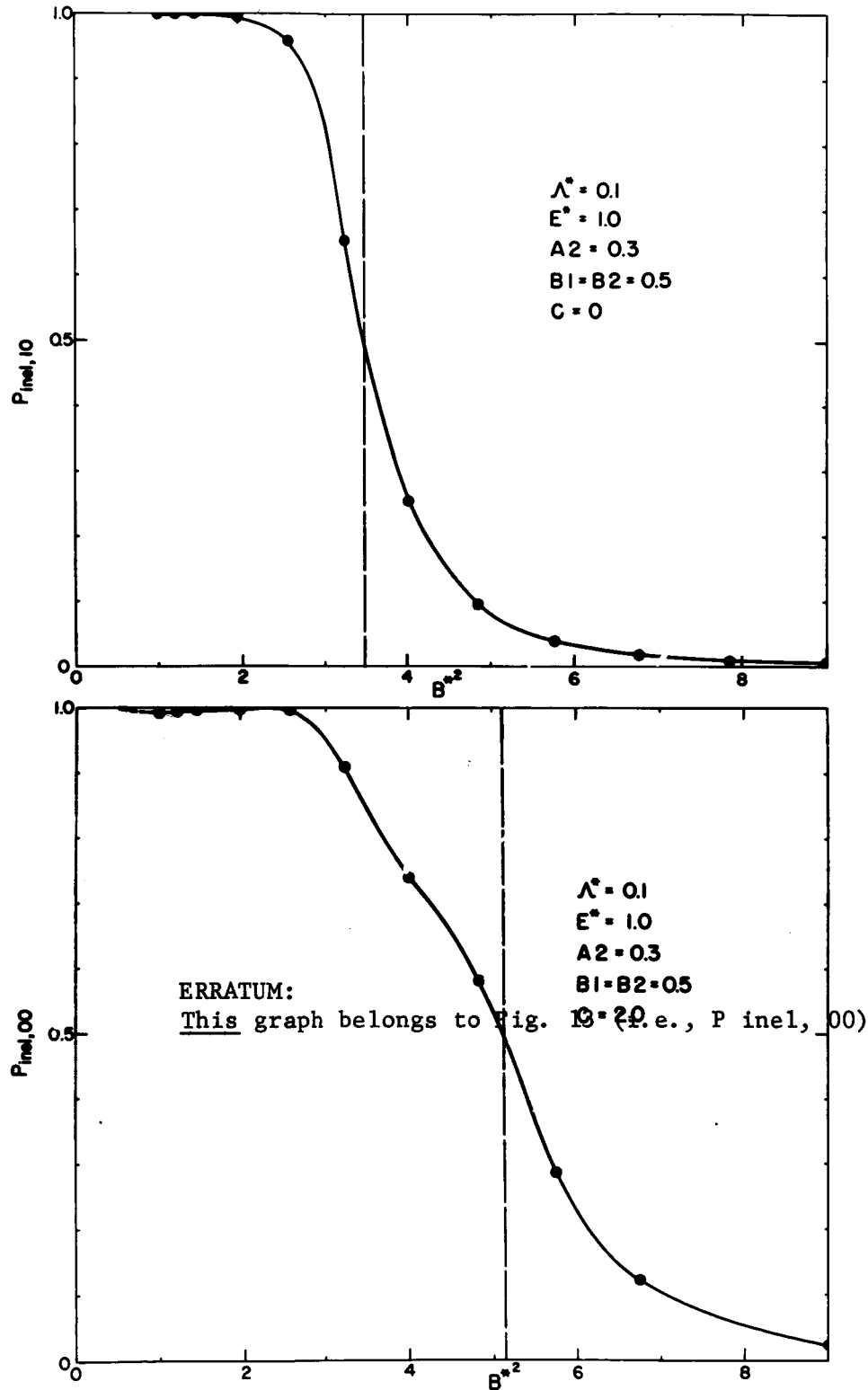


Figure 14

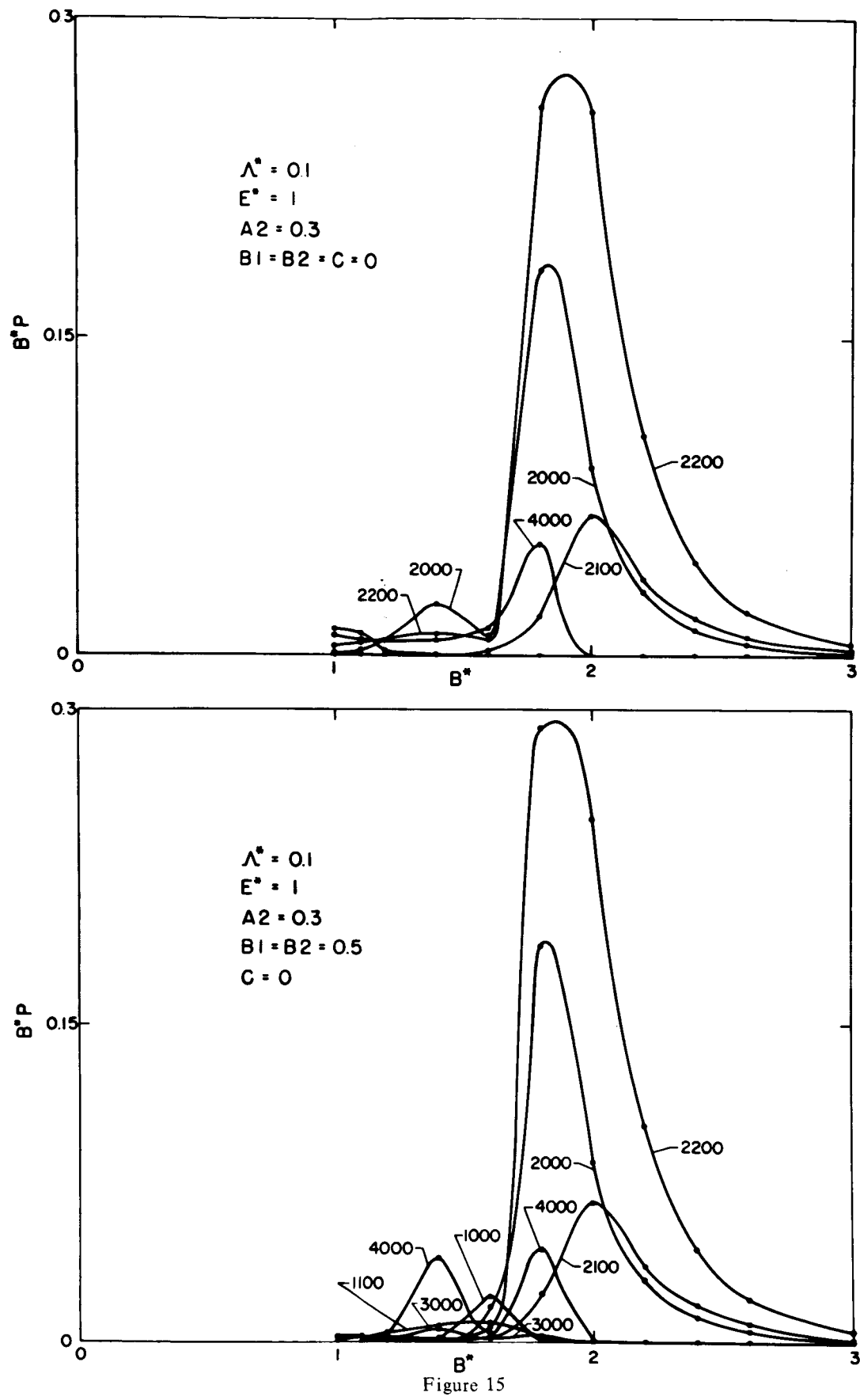


Figure 15

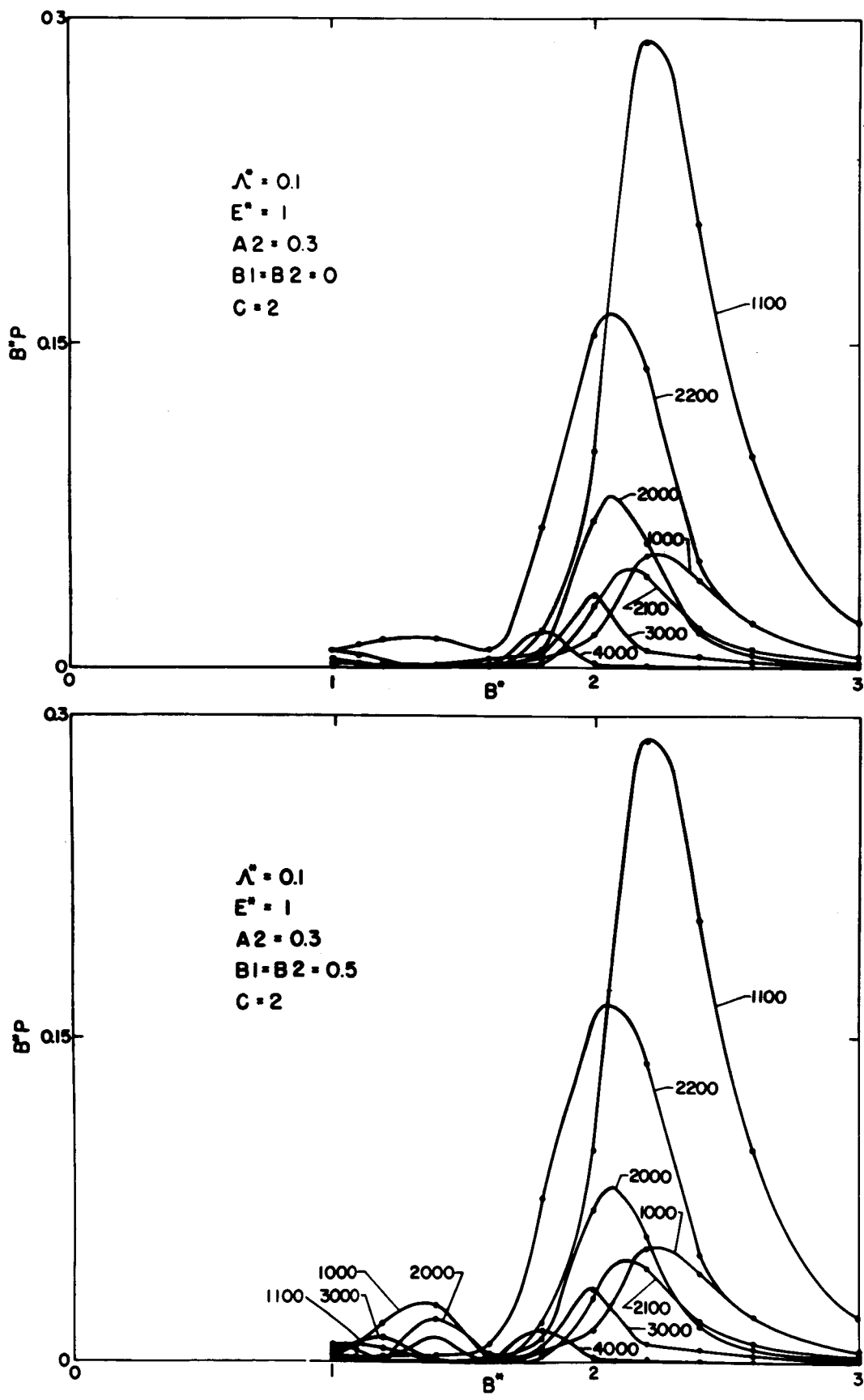
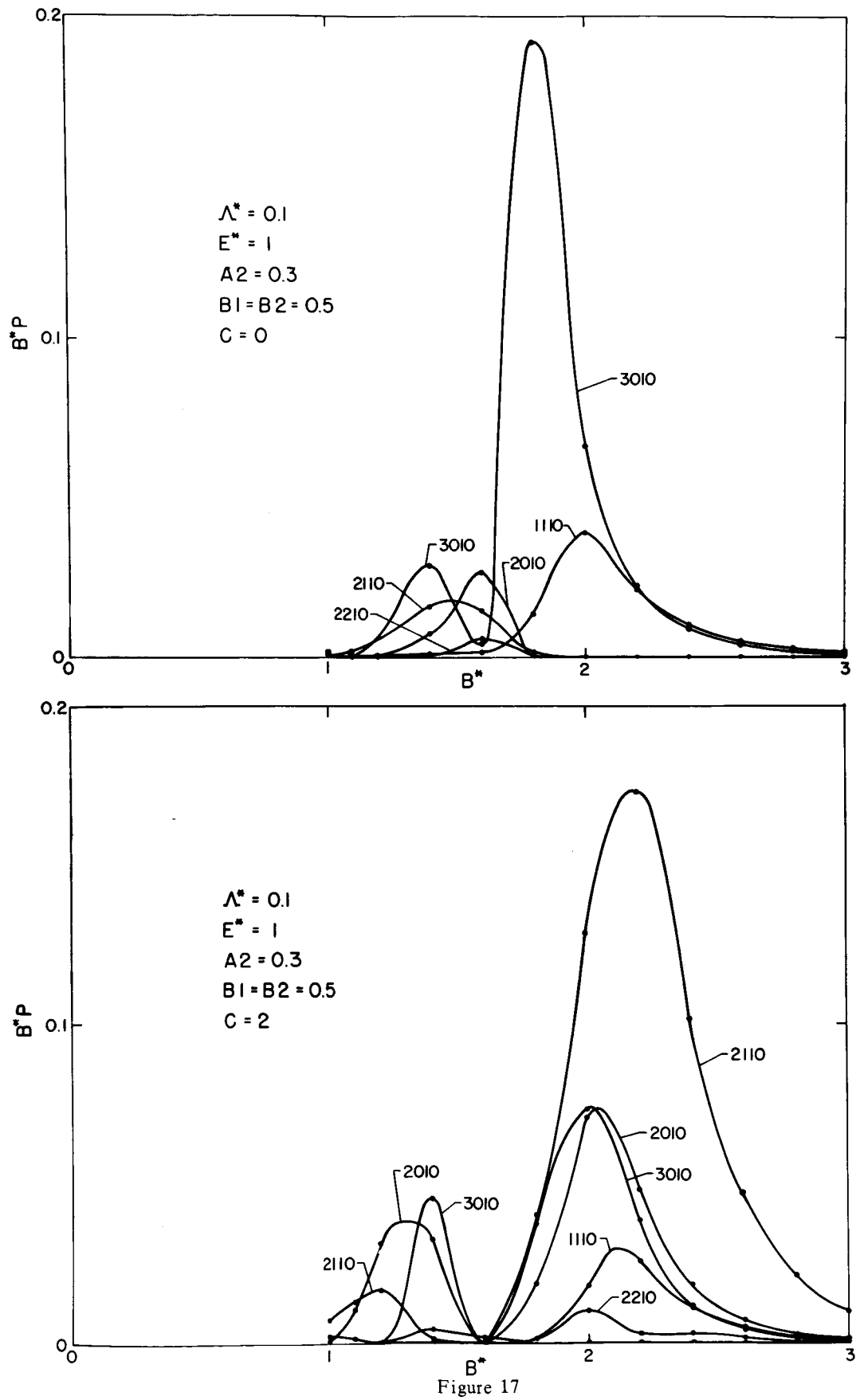


Figure 16



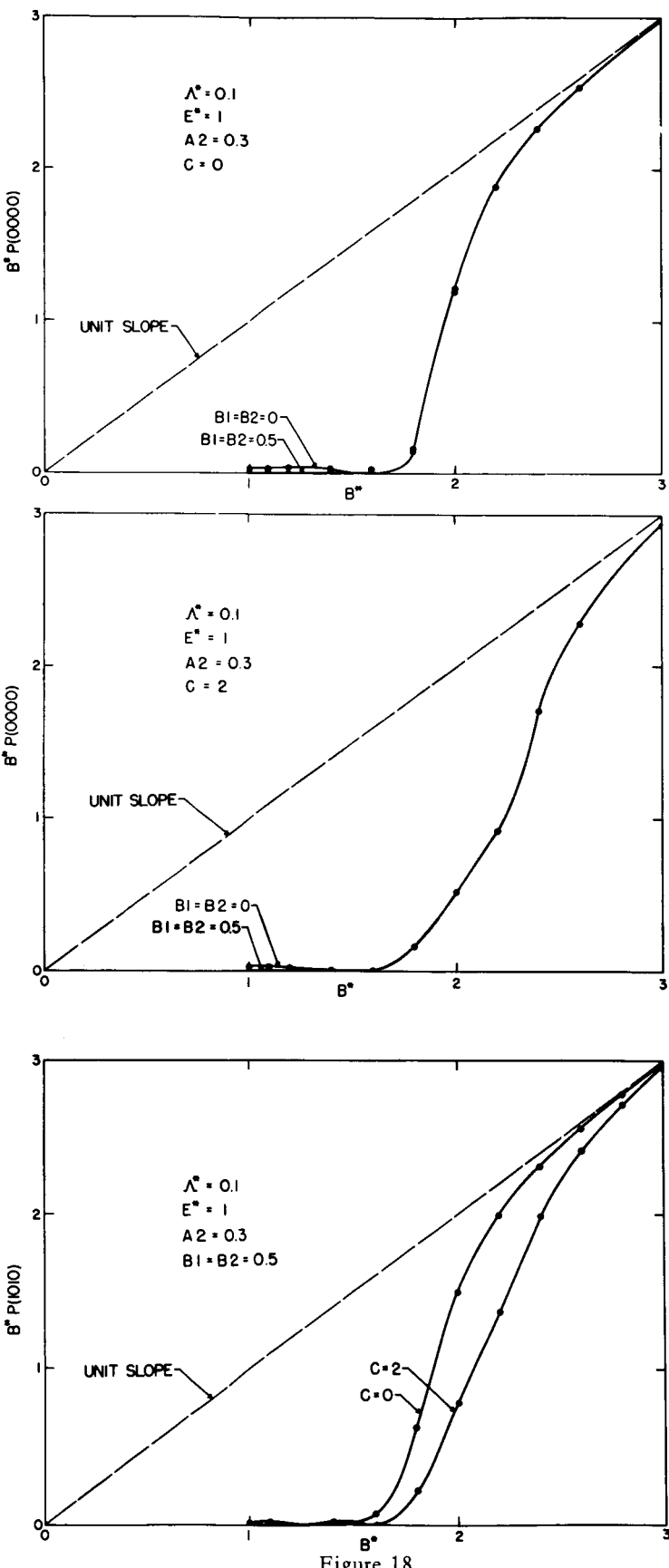


Figure 18

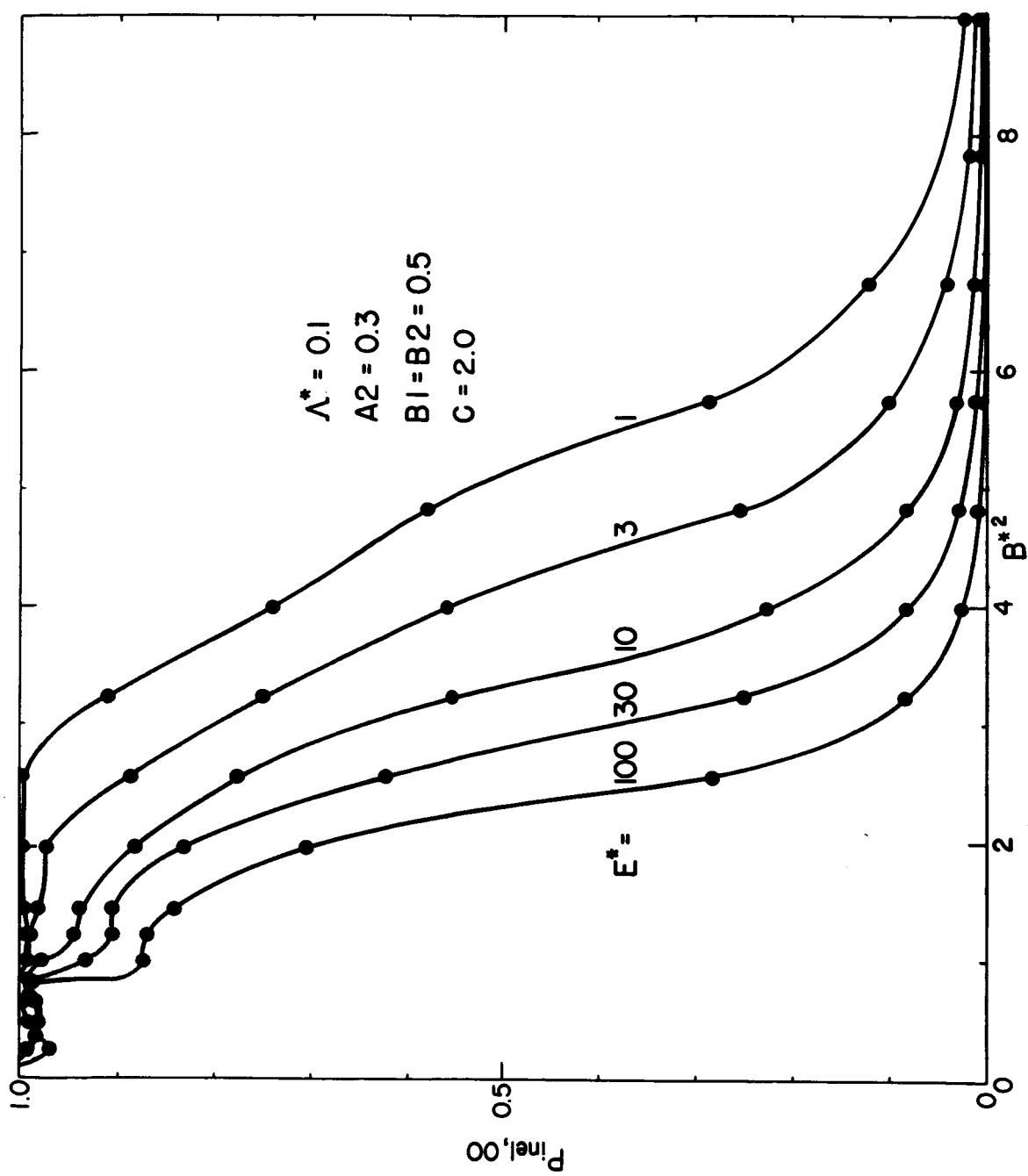


Figure 19

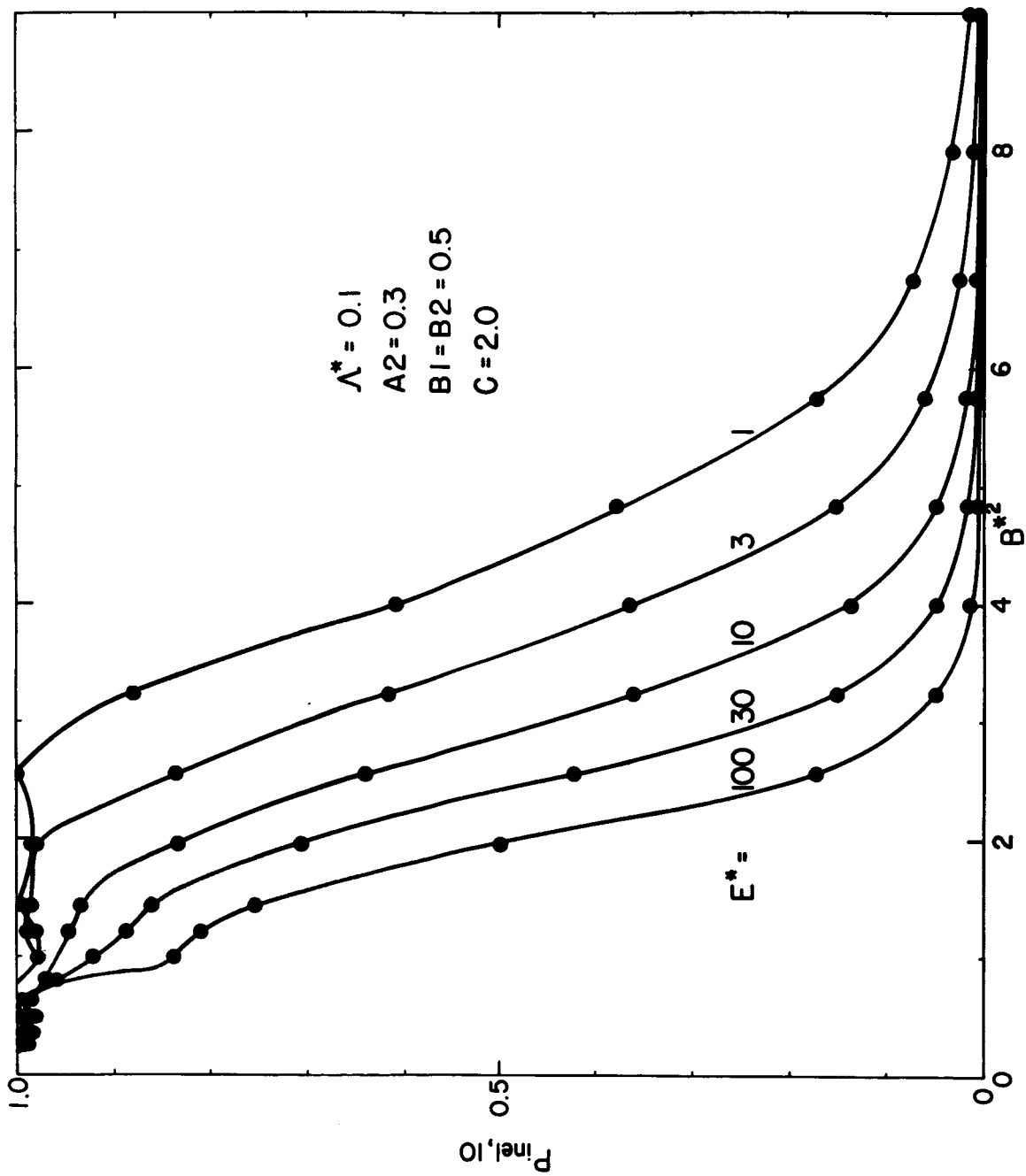


Figure 20

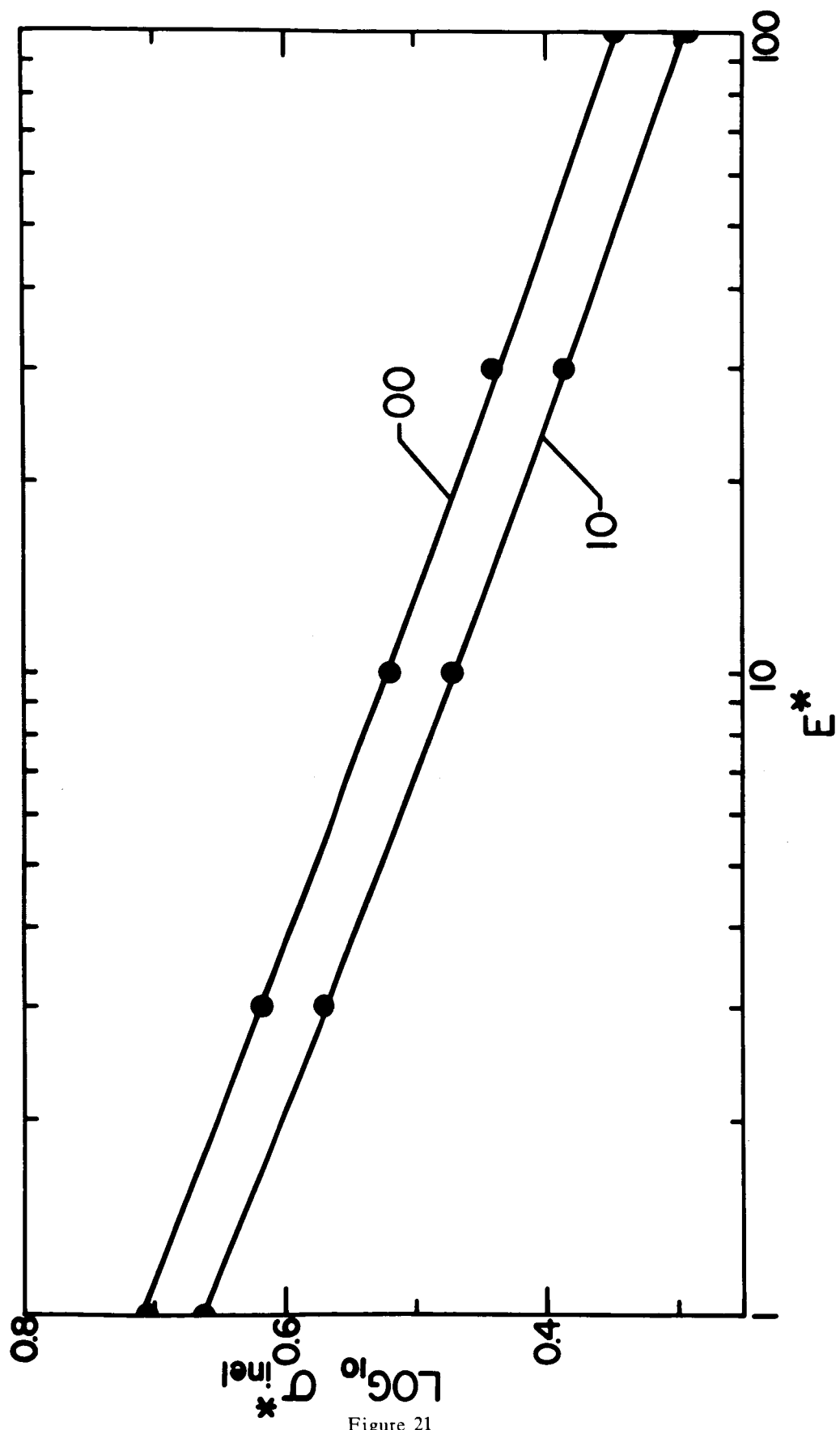


Figure 21

## APPENDIX I

The conversion factors relating the  $I(n,p,q)$  to the  $I_{lm}^{(n)}$   
are as follows:

$$I_{oo}^{(12)} / I(12,0,0) = I_{10}^{(12)} / I(12,1,0) = I_{oo}^{(6)} / I(6,0,0) = I_{10}^{(7)} / I(7,1,0) = 1$$

$$I_{11}^{(12)} / I(12,0,1) = I_{11}^{(7)} / I(7,0,1) = -\sqrt{\frac{3}{2}}$$

$$I_{21}^{(12)} / I(12,1,1) = I_{21}^{(6)} / I(6,1,1) = -\sqrt{\frac{3}{2}}$$

$$I_{22}^{(12)} / I(12,0,2) = I_{22}^{(6)} / I(6,0,2) = \frac{1}{2}\sqrt{\frac{3}{2}}$$

$$I_{32}^{(7)} / I(7,1,2) = \frac{1}{2}\sqrt{\frac{15}{2}}$$

$$I_{33}^{(7)} / I(7,0,3) = -\frac{\sqrt{5}}{4} \quad (\text{AI.1})$$

Asymptotic forms of the  $I(n,p,q)$  integrals are as follows:

$$I(6,0,0) \sim \frac{3\pi}{8} b^{*-5}$$

$$I(6,0,2) \sim \frac{5\pi}{16} b^{*-5}$$

$$I(7,0,1) \sim \frac{5\pi}{16} b^{*-6}$$

$$I(7,0,3) \sim \frac{35\pi}{128} b^{*-6}$$

$$I(12,0,0) \sim \frac{63\pi}{256} b^{*-11}$$

$$I(12,0,1) \sim \frac{512}{693} b^{*-11}$$

$$I(12,0,2) \sim \frac{231\pi}{1024} b^{*-11} \quad (\text{AI.2})$$

The other five integrals vanish in the "straight-line" approximation.

In the limit of small  $b^*$  and high  $E^*$ ,  $G(\theta, \phi)$  becomes independent of  $b^*$  and approaches the simple form

$$G(\theta, \phi) \sim \frac{E^{* \frac{1}{2}}}{b^*} [1 + b_1 P_1(\cos \theta) + b_2 P_2(\cos \theta)] \quad (\text{AI.3})$$

independent of the long range anisotropies  $a_2$  and  $c$ .

**APPENDIX II**

The angular functions  $f_{\beta\alpha}(\theta)$  used in connection with the computation of the matrix elements (Eq. 23) are as follows:

$\beta (= j', m')$	$\alpha (= j, m)$	$f_{\beta\alpha}(\theta)$
0 0 0 0		$\frac{1}{4\pi}$
1 0 0 0	$\theta \sin^2 \theta {}^2_{200} \frac{\sqrt{3}}{5} \frac{1}{\pi^2}$	$\frac{\sqrt{3}}{4\pi} \cos \theta$
1 1 0 0	$\theta^2 \sin^2 \theta {}^2_{200} \frac{\sqrt{3}}{5} \frac{1}{\pi^2}$	$\frac{1}{4\pi} \frac{\sqrt{3}}{2} \sin \theta$
2 0 0 0	$[\theta {}^2_{200} \frac{\sqrt{3}}{5} - \theta {}^4_{200} \frac{2}{5}] \frac{\sqrt{15}}{16} \frac{1}{\pi^2}$	$\frac{\sqrt{15}}{8\pi} (3 \cos^2 \theta - 1)$
2 1 0 0		$\frac{1}{4\pi} \frac{\sqrt{15}}{2} \sin \theta \cos \theta$
2 2 0 0		$\frac{1}{8\pi} \frac{\sqrt{15}}{2} \sin^2 \theta$
3 0 0 0		$\frac{\sqrt{17}}{8\pi} [5 \cos^3 \theta - 3 \cos \theta]$
4 0 0 0		$\frac{3}{32\pi} [35 \cos^4 \theta - 30 \cos^2 \theta + 3]$

$\beta (\equiv j', m')$	$\alpha (\equiv j, m)$	$f_{\beta \alpha} (\theta)$
1 0	1 0	$\frac{3}{4\pi} \cos^2 \theta$
1 1	1 0	$\frac{3}{8\pi} \sqrt{2} \cos \theta \sin \theta$
2 0	1 0	$\frac{1}{8\pi} \sqrt{15} [3 \cos^3 \theta - \cos \theta]$
2 1	1 0	$\frac{3}{4\pi} \sqrt{\frac{5}{2}} \cos^2 \theta \sin \theta$
2 2	1 0	$\frac{3}{8\pi} \sqrt{\frac{5}{2}} \cos \theta \sin^2 \theta$
3 0	1 0	$\frac{1}{8\pi} \sqrt{21} [5 \cos^4 \theta - 3 \cos^2 \theta]$

## APPENDIX III

The double integrals (Eq. 23) were obtained by Simpson's rule quadrature with interval size chosen to be small compared to the "wavelength" of the oscillations of the integrand. Typically, 600-800 intervals were used for each of the variables over their angular ranges  $0 \leq \theta \leq \pi$ ,  $0 \leq \phi \leq 2\pi$ , with a sufficient number of convergence checks being made to demonstrate the significance of the number of figures quoted.

## APPENDIX IV

Tables AIV 1-12 list computed values of the action integrals  $I(n,p,q)$ ; Table AIV 13 gives results for  $y_o$  and Table AIV 14 lists values for  $\chi$ .

The computations were carried out as follows. For a given  $b^*$  and  $E^*$  the root  $y_o$  was determined by the Newton-Raphson method; then the cumulative integrals  $\theta'(y)$  and  $I(n,p,q,y)$  were evaluated (in parallel) by trapezoidal summation from  $y = 0$ , using an appropriate variable interval schedule (typically, the total number of intervals used was 3,000) until  $y$  reached  $y_o$ . Then from  $\theta'(y_o)$  and  $I(n,p,q,y_o)$  the desired values of  $\chi$  and  $I(n,p,q)$  were printed out.

The results for  $\chi$  and  $I(n,p,q)$  are believed to be accurate to within  $\pm 0.0007$  of the values listed. Fig. AIV 1 shows the deflection angle  $\chi(b^*)$  as a function of  $E^*$ .

Table A IV-1  
I(6,0,0)

Table A IV-2  
I(6,0,2)

Table AIV-3

Table I (7,0,1)

Table AIV-5  
I(7,0,3)

Table A IV-6  
I(7,1,0)

Table AIV-7

Table AIV-8  
I(12,0,0)

Table A IV-9  
1(12,0,1)

Table AIV-10  
I(12,0,2)

				1	2	3	5	10	20	30	50	100
E*	B*											
0.01	•00002	•00003	•00005	•00008	•00014	•00027	•00040	•00066	•00132			
•02	•00009	•00015	•00021	•00032	•00058	•00110	•00162	•00266	•00531			
•05	•00057	•00097	•00133	•00202	•00367	•00690	•01012	•01661	•03315			
•10	•00231	•00389	•00534	•00808	•01463	•02745	•04024	•06599	•13151			
•20	•00919	•01543	•02113	•03188	•05750	•10737	•15695	•25643	•50843			
•30	•02046	•03419	•04665	•07007	•12542	•23233	•33791	•54848	•107732			
•40	•03580	•05944	•08071	•12033	•21297	•38962	•56235	•90329	•1.74697			
•50	•05479	•09013	•12154	•17936	•31230	•56091	•79999	•1.26455	•2.38681			
•60	•07682	•12488	•16679	•24259	•41276	•72132	•1.01068	•1.55785	•2.82635			
•70	•10116	•16184	•21341	•30422	•50040	•83904	•1.14250	•1.69171	•2.87426			
•80	•12685	•19874	•25742	•35663	•55747	•87518	•1.13843	•1.57469	•2.38570			
•90	•15272	•23262	•29380	•38993	•56189	•79079	•95073	•1.17252	•1.48312			
•95	•16529	•24726	•30717	•39550	•53707	•69645	•79148	•90513	•1.03367			
1.00	•17733	•25968	•31595	•39120	•49076	•57293	•60988	•64449	•67430			
1.05	•18859	•26919	•31897	•37505	•42266	•43521	•43347	•42863	•42255			
1.10	•19881	•27502	•31470	•34476	•33747	•30457	•30457	•27283	•26077			
1.15	•20764	•27617	•30165	•29881	•24604	•19958	•18328	•17046	•16117			
1.20	•21470	•27153	•27767	•23842	•16425	•12596	•11479	•10653	•10075			
1.25	•21956	•25958	•24062	•17022	•10313	•87868	•87868	•87207	•86394			
1.30	•22166	•23862	•18972	•10807	•06329	•04948	•04948	•04579	•04312			
1.35	•22034	•20608	•12908	•06371	•03902	•03159	•02957	•02810	•02706			
1.40	•21478	•15964	•07434	•03705	•02449	•02053	•01943	•01861	•01803			
1.50	•18573	•04916	•02146	•01356	•01032	•00915	•00881	•00855	•00836			
1.60	•11766	•01183	•00749	•00565	•00472	•00435	•00423	•00415	•00408			
1.70	•01927	•00408	•00313	•00261	•00231	•00218	•00214	•00211	•00208			
1.80	•00353	•00173	•00146	•00129	•00119	•00114	•00113	•00111	•00111			
1.90	•00127	•00083	•00074	•00068	•00064	•00062	•00061	•00061	•00061			
2.00	•00057	•00043	•00040	•00037	•00036	•00035	•00035	•00034	•00034			
2.20	•00015	•00013	•00013	•00012	•00012	•00012	•00012	•00012	•00012			
2.40	•00005	•00005	•00004	•00004	•00004	•00004	•00004	•00004	•00004			
2.60	•0.00002	•0.00002	•0.00001	•0.00001	•0.00001	•0.00001	•0.00001	•0.00001	•0.00001			
2.80	0	0	0	0	0	0	0	0	0			
3.00	0	0	0	0	0	0	0	0	0			
4.00	0	0	0	0	0	0	0	0	0			
4.50	0	0	0	0	0	0	0	0	0			
5.00	0	0	0	0	0	0	0	0	0			

Table A IV - 11  
I(12,1,0)

Table A IV-12  
I(12,1,1)

Table AIV-13  
 $\gamma_0$

$E^*$	1	2	3	5	10	20	30	50	100
<b>B*</b>									
•01	•01032	•01053	•01069	•01095	•01136	•01186	•01219	•01263	•01329
•02	•02064	•02106	•02139	•02190	•02273	•02373	•02438	•02527	•02659
•05	•05159	•05266	•05348	•05474	•05682	•05931	•06094	•06316	•06645
•10	•10316	•10529	•10694	•10944	•11359	•11854	•12179	•12621	•13278
•20	•20616	•21033	•21357	•21849	•22666	•23643	•24282	•25154	•26447
•30	•30883	•31487	•31956	•32673	•33866	•35293	•36227	•37501	•39388
•40	•41099	•41861	•42456	•43369	•44893	•46720	•47917	•49545	•51954
•50	•51245	•52124	•52816	•53882	•55671	•57821	•59227	•61137	•63947
•60	•61300	•62339	•62984	•64143	•66098	•68452	•69987	•72063	•75083
•70	•71237	•72157	•72897	•74059	•76033	•78408	•79947	•82001	•84918
•80	•81027	•81819	•82467	•83498	•85263	•87372	•88711	•90448	•92772
•90	•90631	•91140	•91568	•92258	•93446	•94827	•95659	•96660	•97832
•95	•95349	•95638	•95884	•96286	•96977	•97754	•98197	•98696	•99222
1.00	1.00000	1.00000	1.00000	1.00000	1.00000	1.00000	1.00000	1.00000	1.00000
1.05	1.04576	1.04199	1.03865	1.03310	1.02385	1.01492	1.01077	1.00689	1.00361
1.10	1.09066	1.08200	1.07413	1.06093	1.04001	1.02262	1.01559	1.00957	1.00485
1.15	1.13456	1.11952	1.10544	1.08177	1.04781	1.02469	1.01649	1.00988	1.00492
1.20	1.17730	1.15385	1.13107	1.09351	1.04821	1.02339	1.01536	1.00910	1.00450
1.25	1.21867	1.18389	1.14866	1.09456	1.04386	1.02063	1.01346	1.00794	1.00391
1.30	1.25838	1.20785	1.15465	1.08605	1.03763	1.01755	1.01144	1.00674	1.00332
1.35	1.29605	1.22256	1.14533	1.07269	1.03136	1.01467	1.00957	1.00565	1.00278
1.40	1.33111	1.22202	1.12258	1.05919	1.02582	1.01216	1.00796	1.00470	1.00232
1.50	1.38945	1.15111	1.07538	1.03845	1.01742	1.00834	1.00548	1.00325	1.00161
1.60	1.41333	1.08373	1.04716	1.02548	1.01190	1.00577	1.00381	1.00226	1.00112
1.70	1.18846	1.05154	1.03104	1.01738	1.00829	1.00405	1.00268	1.00160	1.00079
1.80	1.08950	1.03407	1.02127	1.01217	1.00588	1.00289	1.00192	1.00114	1.00057
1.90	1.05552	1.02356	1.01502	1.00871	1.00425	1.00210	1.00139	1.00083	1.00041
2.00	1.03751	1.01683	1.01087	1.00636	1.00312	1.00155	1.00103	1.00061	1.00030
2.20	1.01941	1.00918	1.00602	1.00356	1.00176	1.00087	1.00058	1.00035	1.00017
2.40	1.01105	1.00535	1.00353	1.00210	1.00104	1.00052	1.00034	1.00020	1.00010
2.60	1.00669	1.00328	1.00217	1.00129	1.00064	1.00032	1.00021	1.00012	1.00006
2.80	1.00423	1.00209	1.00139	1.00083	1.00041	1.00020	1.00013	1.00008	1.00004
3.00	1.00278	1.00138	1.00091	1.00054	1.00027	1.00013	1.00009	1.00005	1.00002
3.50	1.00109	1.00054	1.00036	1.00021	1.00010	1.00005	1.00003	1.00002	1.00001
4.00	1.00048	1.00024	1.00016	1.00009	1.00004	1.00002	1.00001	1.00000	1.00000
4.50	1.00024	1.00012	1.00008	1.00004	1.00002	1.00001	1.00000	1.00000	1.00000
5.00	1.00012	1.00006	1.00004	1.00002	1.00001	1.00000	1.00000	1.00000	1.00000

Table AIV-14  
CHI

E*	1	2	3	5	10	20	30	50	100
<b>B*</b>									
.01	3.12220	3.12075	3.11993	3.11890	3.11751	3.11607	3.11520	3.11407	3.11245
.02	3.10281	3.09992	3.09827	3.09622	3.09342	3.09055	3.08881	3.08654	3.08331
.05	3.04461	3.03738	3.03326	3.02812	3.02113	3.01394	3.00959	3.00392	2.99583
.10	2.94751	2.93301	2.92474	2.91445	2.90043	2.88602	2.87729	2.86590	2.94968
.20	2.75244	2.72316	2.70648	2.68569	2.65736	2.62822	2.61056	2.58751	2.55461
.30	2.55536	2.51074	2.48529	2.45359	2.41037	2.36585	2.33884	2.30354	2.25304
.40	2.35517	2.29430	2.25954	2.21624	2.15721	2.09631	2.05929	2.01084	1.94133
.50	2.15062	2.07216	2.02731	1.97143	1.89524	1.81657	1.76869	1.70588	1.61550
.60	1.94025	1.84232	1.78626	1.71645	1.62130	1.52315	1.46339	1.38492	1.27200
.70	1.72231	1.60227	1.53343	1.44781	1.33154	1.21223	1.13996	1.04541	91046
.80	1.49457	1.34870	1.26491	1.16096	1.02147	88107	79752	69090	54565
.90	1.25414	1.07704	97515	85001	68740	53357	44869	34913	23204
.95	1.12796	93251	81994	668331	51179	36158	28582	20460	12186
1.00	99699	78067	65623	50801	33353	20172	14519	9341	4961
1.05	86046	62016	48244	32373	15948	66732	39359	2055	90899
1.10	71737	44912	29688	13210	00229	-0.02808	-0.02602	-0.01901	-0.01058
1.15	56655	26523	09748	-0.06065	-0.11826	-0.08105	-0.05774	-0.03585	-0.01811
1.20	40641	06531	-11629	-0.23865	-0.18677	-0.10038	-0.06731	-0.04023	-0.01980
1.25	23489	-15462	-34047	-0.36912	-0.20564	-0.10011	-0.06557	-0.03859	-0.01878
1.30	04918	-39980	-55575	-0.41878	-0.19419	-0.09087	-0.05902	-0.03453	-0.01672
1.35	-15471	-67274	-70121	-0.39525	-0.17016	-0.07883	-0.05110	-0.02684	-0.01440
1.40	-38285	-95793	-70039	-0.33838	-0.14399	-0.06687	-0.04338	-0.02532	-0.01219
1.50	-95610	-99837	-46532	-0.22638	-0.09949	-0.46389	-0.3051	-0.1780	-0.0850
1.60	-1.90362	-54432	-28848	-0.15040	-0.06844	-0.03269	-0.02131	-0.01240	-0.00585
1.70	-1.62163	-32293	-18744	-0.10225	-0.04789	-0.02295	-0.01495	-0.00866	-0.00399
1.80	-61393	-20864	-12705	-0.07124	-0.03391	-0.01629	-0.01058	-0.00607	-0.00271
1.90	-35692	-14214	-0.08895	-0.05096	-0.02438	-0.0169	-0.00755	-0.00426	-0.00182
2.00	-23352	-1039	-0.06386	-0.03701	-0.01777	-0.00847	-0.00542	-0.00299	-0.00118
2.20	-11690	-0.05413	-0.03506	-0.02042	-0.00977	-0.00454	-0.00281	-0.00144	-0.00041
2.40	-0.06534	-0.03116	-0.02029	-0.01180	-0.00554	-0.00245	-0.00143	-0.00061	-0.0001
2.60	-0.03920	-0.01881	-0.01223	-0.00704	-0.00319	-0.00128	-0.00065	-0.00014	24
2.80	-0.02450	-0.01175	-0.00759	-0.00428	-0.00183	-0.00060	-0.00019	-0.00013	37
3.00	-0.01583	-0.00752	-0.00479	-0.00262	-0.00100	-0.00019	-0.00008	-0.00002	46
3.50	-0.00584	-0.00529	-0.00152	-0.00066	-0.00002	-0.00000	-0.00000	-0.00000	55
4.00	-0.00227	-0.00082	-0.00034	-0.00004	-0.00000	-0.00000	-0.00000	-0.00000	59
4.50	-0.00080	-0.00009	-0.00014	-0.00033	-0.00048	-0.00055	-0.00057	-0.00059	60
5.00	-0.00014	-0.00024	-0.00037	-0.00417	-0.00054	-0.00058	-0.00059	-0.00060	61

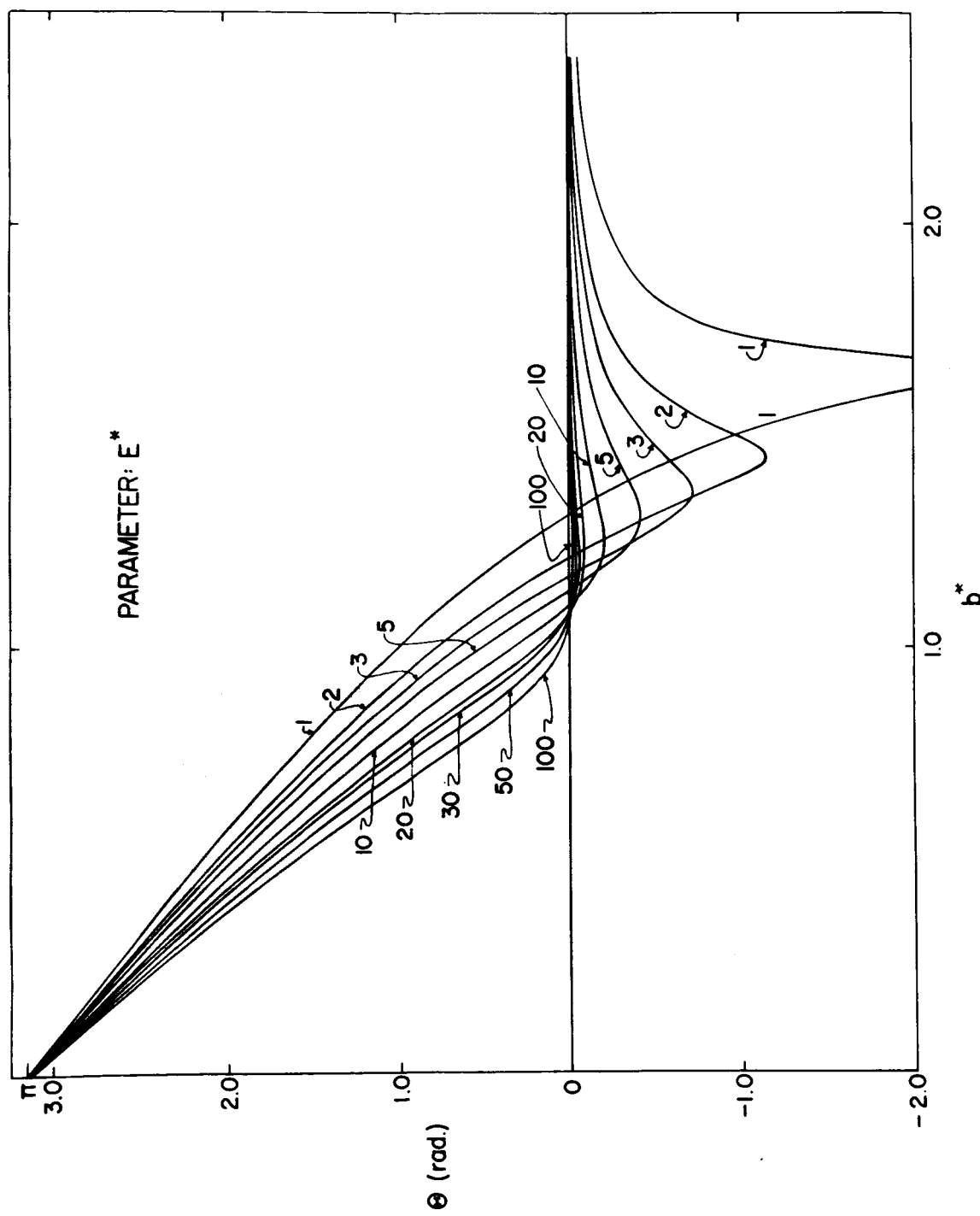


Figure 1 AII

ERRATUM: Figure No. is AIV 1

## APPENDIX V

The tables of computed transition probabilities are too extensive to be included in this report. They are presented in an auxiliary document (WIS-TCI-91G), available on request. Table AV.1 of the latter refers to transitions from the 0,0 state, while Table AV 2 lists those from the 1,0 state. The energy dependencies of  $P(0000)$  and  $P(1010)$  are summarized in Table AV3.

The difficulty in obtaining convergence in the integration for the transition probability (Eq. 23) increases drastically as the product  $\sqrt{E}^{\frac{1}{2}}$  is decreased below about 0.1 and as  $b^*$  is decreased below about 0.9, due to the increasingly oscillatory behavior of the integrand. This consideration has influenced the choice of the range of the variables studied and the number of significant figures quoted in the results.

WIS-TCI-91 Erratum, Sept. 24, 1965

"SUDDEN APPROXIMATION APPLIED TO ROTATIONAL EXCITATION OF  
MOLECULES BY ATOMS. II. SCATTERING OF POLAR DIATOMICS"

by

R. B. Bernstein and K. H. Kramer

An error has been discovered in the expression for the action which may have serious implications with respect to the computed transition probabilities and inelastic cross sections.

Eqs. 14, 17 and 20 imply for the action a symmetry about the apse line which is not justified; i.e.,  $I(-\infty, \infty) \neq 2 I(0, \infty)$ . The discrepancy is most important for the five action integrals which vanish in the "straight-line" approximation.

Until further work (now in progress) has clarified (and corrected) this difficulty, the validity of the computed results must be considered in doubt. However, it is likely that most of the qualitative conclusions of the Report will remain unaltered.